National Library of Canada
Acquisitions and Bibliographic Services Branch
395 Wellington Street
Ottawa, Ontario
K1A 0N4

Bibliothèque nationale du Canada
Direction des acquisitions et des services bibliographiques
395, rue Wellington
Ottawa (Ontario)
K1A 0N4

Your file Votre référence

Our file Notre référence

NOTICE

The quality of this microform is heavily dependent upon the quality of the original thesis submitted for microfilming. Every effort has been made to ensure the highest quality of reproduction possible.

If pages are missing, contact the university which granted the degree.

Some pages may have indistinct print especially if the original pages were typed with a poor typewriter ribbon or if the university sent us an inferior photocopy.

AVIS

La qualité de cette microforme dépend grandement de la qualité de la thèse soumise au microfilmage. Nous avons tout fait pour assurer une qualité supérieure de reproduction.

S'il manque des pages, veuillez communiquer avec l'université qui a conféré le grade.

La qualité d'impression de certaines pages peut laisser à désirer, surtout si les pages originales ont été dactylographiées à l'aide d'un ruban usé ou si l'université nous a fait parvenir une photocopie de qualité inférieure.

Canada

A Computational and Experimental Investigation of a Heat Pipe Injection Lance

by

Jonathan H. Kay

Department of Mining and Metallurgical Engineering

McGill University

Montreal, Canada

May, 1994

A thesis submitted to the Faculty of Graduate Studies and Research in partial fulfillment of the requirements for the degree of Master of Engineering

ISBN 0-315-99967-5

Canada

Shortened version of the thesis title :

Investigation of a heat pipe injection lance

- Dedicated to Audrey -

Abstract

The heat pipe is an engineering device capable of transporting large amounts of heat energy. Because a heat pipe is a closed system, contains no moving mechanical components and transports heat over very small temperature gradients, it presents an attractive alternative to conventional forced-convection cooling techniques.

Over the past 4 decades, the principles of heat pipe operation have been thoroughly investigated. Heat pipes have been implemented in a wide variety of engineering applications. Despite this, heat pipes have not been used on a large scale in metallurgical applications. In this regard, an enormous potential for improved efficiency and productivity remains unexploited.

Heat pipe research at the McGill Metals Processing Centre has aimed to correct this. Various metallurgical applications for heat pipe technology have been explored by Mucciardi, Botos, Choi, Jin and Meratian. The research effort has concentrated on gas-loaded annular thermosyphons, a subclass of heat pipes. The work presented in this volume represents the author's contribution to this larger research effort.

A series of experiments has been performed in order to investigate important aspects of the operation of gas-loaded thermosyphons. Results from these experiments were subsequently incorporated into a PC-based computer model for the design and analysis of annular thermosyphons.

Résumé

Le caloduc est un dispositif capable de transporter de grandes quantités de chaleur avec un faible gradient thermique. Un caloduc est un système fermé qui ne contient aucune pièce mobile. Ces caractéristiques en font une alternative attrayante aux modes de refroidissement conventionnels.

Au cours des quatre dernières décennies, les principes d'opération des caluducs ont été étudié à fond par la communauté scientifique. Les caloducs sont utilisés dans une grande variété d'applications dans le domaine du génie mecanique, mais beaucoup moins dans des applications métallurgiques. Présentement, l'industrie métallurgique gaspille ce grand potentiel d'amélioration d'efficacité de productivité.

Un groupe de chercheurs du Centre de Transformation des Métaux de l'Université McGill travaille à corriger cette lacune. Une variété d'applications métallurgiques des calcducs ont été étudié par Mucciardi, Botos, Choi, Jin et Meratian. Les efforts de ces chercheurs se sont concentrés dans le domaine des thermosyphons, un type particulier de caloduc. Les travaux de recherche présentés dans cet ouvrage ne sont qu'un constituant de ce grand effort de recherche mené à l'université McGill.

Un programme d'expérimentation a été mené pour étudier les aspects importants de l'opération des thermosyphons. Les résultats de ces expériences ont été utilisé pour bâtir un logiciel d'analyse de l'opération des thermosyphons.

Acknowledgments

I owe a great deal to Professor Frank Mucciardi for his friendship and counsel. Without Professor Mucciardi's enthusiastic support and tireless assistance, this work would not be possible. Moreover, my daily conversations with Professor Mucciardi were an engaging diversion from the occasionally frustrating task of scientific research.

I would also like to thank my fellow graduate students at the McGill Metals Processing Centre. In particular, I must thank Mahmood Meratian and Ning Jin. If not for their assistance and support, I might still be in the laboratory, my experiments incomplete.

Professor Ralph Harris of the Department of Metallurgical Engineering and Professor Rabi Baliga of the Department of Mechanical Engineering have also contributed significantly to my research effort. I would like to thank them for sharing the benefits of their insight and knowledge.

I would also like to acknowledge the less tangible, but no less significant support which I received from my family. My pursuit of higher education is a product of their encouragement. Finally, there is Audrey, whose presence in my life has been my greatest source of happiness and strength. As modest a work as this may be, it is humbly dedicated to her.

Contents

CONTENTS

Tables

Figures

Nomenclature

a	Fluid parameter for a given material. Governs relationship between gas-phase pressure and temperature at equilibrium.
A_{bottom}	Area exposed for heat transfer at lance tip = $\pi \cdot (r_i^2 - r_c^2)$.
A_{cs}	Cross-sectional area of fluid flow in pipe, m^2.
A_g	Cross-sectional area available to reagent gas flow = $\pi \cdot r_b^2$.
A_k	Cross-sectional area of solid outer shell = $\pi \cdot (r_o^2 - r_i^2)$, m^2.
b	Fluid parameter for a given material. Governs relationship between gas-phase pressure and temperature at equilibrium.
β	Stefan-Boltzmann constant = 5.669×10^{-8} W/($m^2 \cdot K^4$).
B_f	Thermal volumetric expansion coefficient, as measured at the boundary film, 1/°C.
c_o	Molar density of gas/vapor mixture, Kg-mol/m^3.
C_p	Heat capacity of substance, J/kg•°C.
$C_{p,f}$	Heat capacity of the ambient cooling medium, as measured at the boundary film, J/kg•°C.
$C_{p,gas}$	Heat capacity of reagent gas, J/kg•°C.
c_{sf}	Surface-liquid coefficient obtained from experimental data for a given fluid-surface combination.
D	Diffusivity of vapor in inert gas, m^2/s.
δ	Film thickness, m.
ε	Surface emissivity.
E	Peterson's dimensionless diffusion parameter = $c_o \cdot MW_V \cdot D \cdot \kappa / (h_{c,tot} \cdot [T_{sat} - T_{env}] \cdot r_i)$.
F	View factor for radiative heat transfer.
G	Mass of working substance in pipe, kg.
g	Gravitational acceleration = 9.81 m/s^2.
g_c	Proportionality constant = 1 kg•m•N^{-1}•s^{-2}.
h_b	Heat transfer coefficient, boiling regime, W/(m^2•°C).
h_{bottom}	Heat transfer coefficient, environment with lance tip, W/(m^2•°C).
h_{con}	Heat transfer coefficient, condenser with ambient environment, W/(m^2•°C).
$h_{c,tot}$	Heat transfer coefficient, condenser with ambient environment, including linearized radiation contribution, W/(m^2•°C).
h_{gas}	Heat transfer coefficient, reagent gas with inner pipe, W/(m^2•°C).
$h_{i,ext}$	Heat transfer coefficient, ith node, outer periphery of pipe with ambient environment, W/(m^2•°C).

$h_{i,ws}$	Heat transfer coefficient, ith node, heat pipe shell with working substance, W/(m^2•°C).
$h_{tip,ws}$	Heat transfer coefficient at lance tip, heat pipe shell with working substance, W/(m^2•°C).
k_c	Thermal conductivity of the protective coating, W/(m• °C).
k_f	Thermal conductivity of the ambient cooling medium, as measured at the boundary film, W/(m• °C).
k_l	Thermal conductivity of the liquid, W/(m• °C).
k_s	Thermal conductivity of the heat pipe shell, W/(m• °C).
k_{tip}	Thermal conductivity of the heat pipe shell, at lance tip, W/(m• °C).
κ	Heat of vaporization of working substance, J/kg.
l_a	Length of adiabatic section, m.
l_c	Length of active condenser, m.
L_c	Non-dimensionalized active condenser length = l_c/l_t.
l_e	Length of evaporator section, m.
$L^*_{g,ff}$	$l_{ig,ff} / r_i$.
l_i	Vertical length of ith axial segment, m.
$l_{ig,ff}$	Length of blocked off region predicted by flat front model = l_t-l_c, m.
$l_{shut-off}$	Length of blocked off region predicted by 1-D, 2-D Exact, 2-D Integral and 2-D Analytic models, m.
l_t	Total condenser length including blocked off region, m.
m	Mass flow, kg/s.
MW_v	Molecular weight of working substance, g/mol.
μ, μ_l	Dynamic viscosity of working substance liquid, kg/(m•s).
μ_f	Dynamic viscosity of the ambient cooling medium, as measured at the boundary film, kg/(m•s).
ν_f	Kinematic viscosity of the ambient cooling medium, as measured at the boundary film, m^2/s.
n_{ig}	Moles of inert gas contained in the pipe.
P	System pressure, Pa.
P_{gas}	Pressure in reagent gas line, Pa.
P_{ht}	Liquid heat transfer parameter. Used to determine the heat transport capability of a given working substance
P_{ig}	Pressure in inert gas section, Pa.
P_{sat}	Equilibrium vapor pressure of working substance at T_{ws}, Pa.
$P_{sat,env}$	Equilibrium vapor pressure of working substance at T_{env}, Pa.
P_{ws}	Pressure, working substance, Pa.
Pr_{sat}	Prandtl number of saturated liquid.

θ_C	Dimensionless temperature, $T_{env}/(T_{sat}-T_{env})$, ratio calculated with temperatures measured in degrees Kelvin.
$\theta_{Contact}$	Contact angle between liquid droplet and solid surface (degrees).
Q	Quantity of heat, J.
Q^*_g	$l_{shut\text{-}off} / r_i$.
q''	Heat flux, W/m^2.
$q''_{crit,b}$	Critical heat flux of boiling ("boiling limit"), W/m^2.
$q_{i,a}$	Energy transfer from environment to working substance, ith node, W.
$q_{i,b}$	Energy expelled from working substance to reagent gas, ith node, W.
q_{tip}	Energy transfer from environment to working substance, lance tip, W.
q_{tot}	Heat load on the pipe, W.
R	Gas constant = 8.314 N•m/(mol•K).
r_b	Inner radius of inner pipe, m.
r_c	Outer radius of inner pipe, m.
r_i	Internal radius of heat pipe outer shell, m.
$r_{i,e}$	Inner radius of outer pipe, ith nodal ring, m.
$r_{i,f}$	Outer radius of outer pipe, ith nodal ring, m.
$r_{i,g}$	Outer radius of protective refractory, ith nodal ring, m.
r_o	Outer radius of heat pipe outer shell, m.
ρ_{ig}	Density of inert gas, kg/m^3.
$\rho_{ig,atm}$	Density of inert gas at S.T.P., kg/m^3.
ρ_l	Density of liquid, kg/m^3.
ρ_r	Density of reagent gas, kg/m^3.
ρ_v	Density of vapor, kg/m^3.
$\rho_{v,atm}$	Density of vapor at atmospheric boiling point, kg/m^3.
σ	Surface tension of liquid-vapor interface, N/m.
S	Periphery of outer wall of outer pipe, m.
t_c	Thickness of coating at lance tip, m..
t_s	Thickness of pipe shell at lance tip, m..
$T_\bullet$	$(1-T_{sat}/T_{env})^{-1} \bullet \ln(P_{sat,env}/P_{sat})$.
$T_{amb,i}$	Temperature of external environment, ith node, K.
$T_{b,a}$	Temperature of pipe bottom, exposed coating surface, K.
$T_{b,b}$	Temperature of pipe bottom, inner edge of protective coating, K.
$T_{b,c}$	Temperature of pipe bottom, inner edge in contact with working substance, K.
T_{env}	Temperature of the ambient environment, K.
$T_{env,tip}$	Temperature of the ambient environment, lance tip, K.
$T_{i,a}$	Bulk temperature of reagent gas, ith node, K.
$T_{i-1,a}$	Bulk temperature of reagent gas, node I-1 (node above ith node), K.

$T_{i,b}$	Temperature of inner wall of inner pipe, ith node, K.
$T_{i,c}$	Temperature of outer wall of inner pipe, ith node, K.
$T_{i,e}$	Temperature of inner wall of outer pipe, ith node, K.
$T_{i,f}$	Temperature of inner wall of protective coating / outer wall of outer pipe, ith node, K.
$T_{i,g}$	Temperature of outer wall of protective coating, ith node, K.
T_{gas}	Temperature of the reagent gas, K.
T_s	Temperature of surface, K.
T_{sat}	Saturation temperature of vapor, K.
T_{ws}	Temperature of working substance, K.
$T_{ws,e}$	Temperature of the working substance in the evaporator, K.
v_g	Velocity of reagent gas.
V_{ig}	Volume consumed by inert gas plug, m^3.
W	Peterson's dimensionless wall conduction parameter = $k_s \bullet (r_o - r_i)/(r_i^3 \bullet h_{c,tot})$.
Ψ	Bobco's heat load index = $q_{tot}/(h_{c,tot} \bullet S \bullet l_c)$.
z	Index variable for the vertical dimension.
$Z_{b,a}$	Vertical position of the pipe tip, outer surface of protective coating, m.
$Z_{b,b}$	Vertical position of the pipe tip, inner surface of protective coating, m.
$Z_{b,c}$	Vertical position of the pipe tip, inner surface of pipe, m.
Z_{bottom}	Vertical position of the bottom of the pipe, m.
$Z_{f,i}$	Vertical position of the vapor/gas interface (inner pipe wall), m.
$Z_{f,o}$	Vertical position of the vapor/gas interface (outer pipe wall), m.
$Z_{f,\Delta}$	$Z_{f,o} - Z_{f,i}$, m.
Z_{top}	Vertical position of the top of the pipe, m.

1

Introduction

A heat pipe is a device which moves heat from one location to another. Properly employed, the heat pipe can provide decisive advantages over conventional cooling systems such as water sprays and jackets. A heat pipe contains no moving parts and requires no external power or mass input during operation.

While the advantages of heat pipes have been exploited in other engineering applications, most notably the cooling of space satellites, the metallurgical industry has been slow to adopt heat pipe technology. In many ways, all pyrometallurgical operations are predicated on the precise, controllable, safe and inexpensive transfer of heat loads during process steps. It is surprising, therefore, that this segment of industry has done little or no research into such an innovative means of heat evacuation.

One example of an application which will benefit in coming years from the introduction of heat pipe technology is the top-blowing injection lance. Used for BOF steelmaking, copper processing and other applications, the top-blowing injection lance must endure severe thermal boundary conditions. Conventional lances rely on either an elaborate pump-and-channel system of water cooling or disposable "melt-away"

designs. The introduction of the heat pipe injection lance will add a new, more efficient option and open the way for other heat pipe applications in metallurgy.

This work details the author's computational and experimental efforts to investigate the operation of heat pipe injection lances.

Chapter 2 of this volume illustrates the history of the heat pipe. The various types of heat pipes and their applications are discussed. Emphasis is placed on the *gas-loaded annular thermosyphon*, a sub-class of heat pipes which encompasses the heat pipe injection lances presently under study.

Chapter 3 details the engineering science aspects of heat pipe operation with regard to known principles of heat and mass transfer. In Chapter 4, various heat pipe modeling techniques are discussed. Emphasis is placed on the *flat-front* model, a model type which will be used to build the software package discussed in Chapter 6.

Chapter 5 describes the bench-top experiments conducted by the author in order to investigate the behavior of gas-loaded annular thermosyphons. The experimental regime was conceived in order to perform two tasks: 1) To investigate the practical viability of the heat pipe injection lance and 2) To corroborate the simplifying assumptions employed in the mathematical model discussed in Chapter 6.

Chapter 6 illustrates the design and operation of *HEATPIPE 1.0*, a PC-based software package created by the author to perform fast, easy simulation of heat pipe

injection lances. Chapter 7 provides a brief conclusion summarizing the results of the work conducted.

2

The Heat Pipe

2.1 Introduction

A heat pipe is a sealed pipe shell which can be used to transfer large quantities of heat through small surface areas. In the most general case, a heat pipe consists of a sealed pipe shell containing a condensable *working substance*. Figure 2.1 illustrates a basic heat pipe.

During heat pipe operation, one end of the pipe is exposed to a heat source. This end of the pipe is designated the *evaporator*, so named because the heat transmitted through the pipe wall at this point is used to evaporate liquid working substance into the vapor phase. This vapor then follows the small pressure gradient which exists along the pipe's axis, and subsequently condenses at the other end of the pipe - the *condenser*. The latent heat of condensation is released and conducted through the walls of the container and into the external environment. From this point, the working substance condensate returns to the evaporator in liquid form. Often, a capillary wick is required for this function.

Having returned back to the evaporator section, the condensate once again will be vaporized and propelled axially to the condenser. In this way, the liquid and vapor flow form a closed circuit. Net heat transfer is accomplished from the working substance's endothermic evaporation in the evaporator and subsequent exothermic condensation in the condenser.

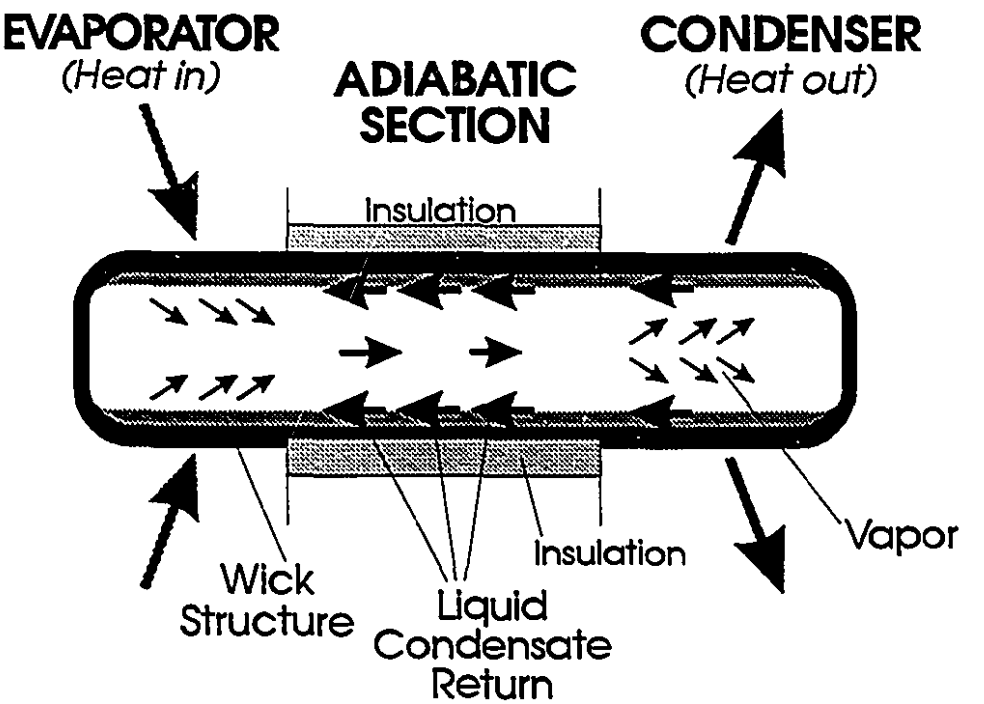

Figure 2.1
Schematic of a Typical Heat Pipe

In between the condenser and the evaporator sections may be situated an insulated *adiabatic* section. In this section, neither condensation nor evaporation take place.

2.2 Advantages of a Heat Pipe

The principal advantage of a heat pipe is that it may transport enormous quantities of heat across a very small pressure gradient. For this reason, heat pipes have been termed "Superconductors of heat" by more than one author[i,ii]. Indeed, it's *effective thermal conductivity* is orders of magnitude more than even the most heat conductive solid metals.

Furthermore, because the latent heat of evaporation for working substances is generally quite high, an enormous amount of heat transfer can be accomplished by means of a very small amount of mass transfer. In a sodium-charged heat pipe for example, one gram of sodium changing phase from liquid to vapor (evaporation) will absorb roughly as much heat energy as 32 grams of sodium undergoing a 100° C temperature increase.

An additional advantage of heat pipes is that the working substance and the various sections of the shell exhibit, individually, virtually perfect isothermal behavior.

> "...The condenser surface of a heat pipe will tend to operate at uniform temperature. If a local heat load is applied, more vapor will condense at this point, tending to maintain the temperature at the original level..." [iii]

When the heat pipe is operating within normal parameters, the working substance vapor and liquid phases are at or very near thermal equilibrium. This fact, coupled with the extremely small pressure gradients within the pipe, give rise to a working substance which is almost completely isothermal.

2.3 Types of Heat Pipes

Heat pipes may be divided broadly according to the mode of vapor / liquid flow within the pipe[iv], the flow regimes being parallel-flow, counter-flow and cross-flow. Heat pipes are also classified according to the mode of condensate return[v]. The various methods of condensate return are listed in table 2.1 Of the listed pipes, the most common and the most robust is the gravity-driven thermosyphon.

Method of Condensate Return	Type of Heat Pipe
Gravity	Thermosyphon
Capillary Force	Standard Heat Pipe
Centrifugal Force	Rotating Heat Pipe
Electrostatic Volume Forces	Electrohydrodynamic Heat Pipe
Magnetic Volume Forces	Magnetohydrodynamic Heat Pipe
Osmotic Forces	Osmotic Heat Pipe
Bubble Pump	Inverse Thermosyphon

Table 2.1
Methods of Condensate Return for Different Types of Heat Pipes

The topic of concentration for the balance of this volume will be counter-flow thermosyphons (gravity heat pipes).

2.3.1 Thermosyphons

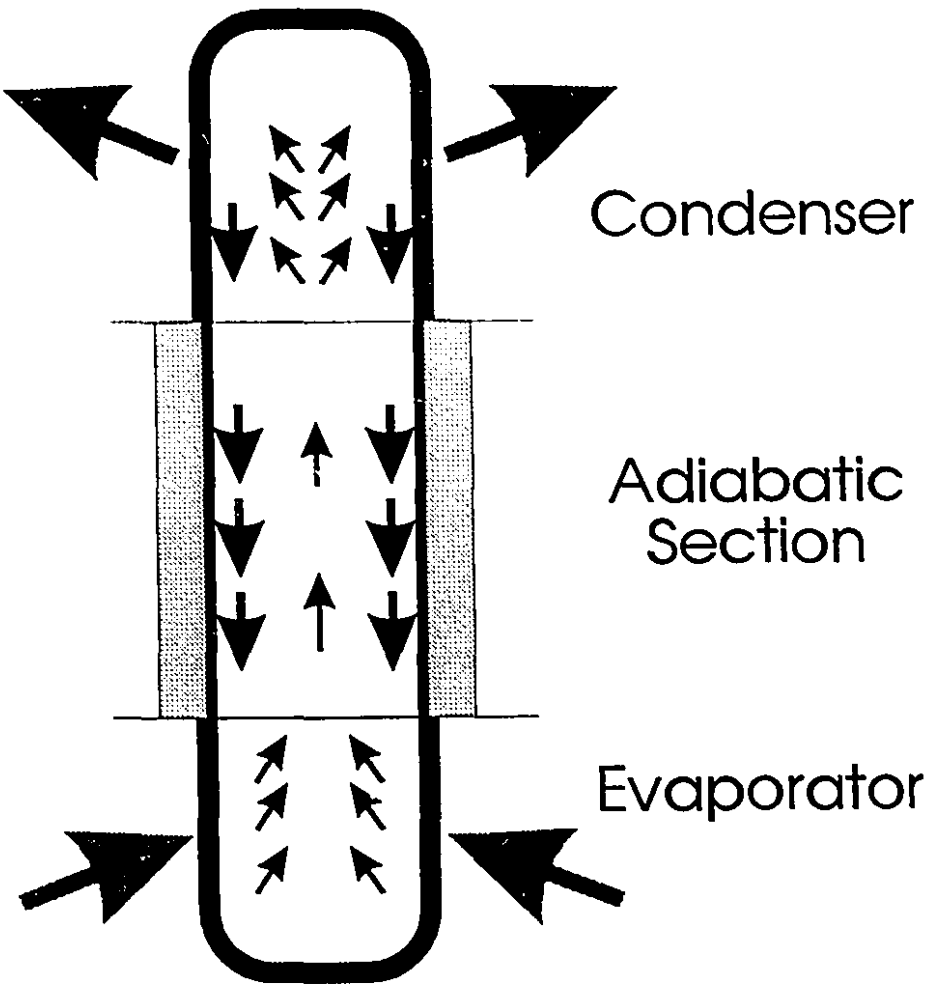

Figure 2.2
Schematic of a Thermosyphon

As indicated in Table 2.1, a thermosyphon is simply a gravity heat pipe. Because there is no wick required to return the condensate to the evaporator section of the pipe, thermosyphons are often termed *wickless heat pipes*.

A schematic of a thermosyphon is presented in Figure 2.2. Because gravity force is necessary to return the condensate to the evaporator, a thermosyphon must be oriented in such a way that the evaporator section is lower than the condenser. This requirement places constraints on the use of thermosyphons. The fact that thermosyphons require no wicks, however, means that they are easier to construct and more robust in operation.

2.3.2 Gas-Loaded Heat Pipes

Gas-loaded heat pipes, (or *VCHP*, Variable Conductance Heat Pipes, as they are better known) were first investigated by Wyatt in 1965[vi]. In 1967, Katzoff[vii] noted that the inclusion of non-condensable gas within a heat pipe could allow effective thermostatic control during operation. In 1971 Marcus[viii] produced a definitive reference on VCHP which outlined their advantages over standard heat pipes.

When a non condensable gas exists in the presence of the working substance, it is swept to the far end of the condenser by the working substance vapor flow. The inert gas is trapped by the convective flow of the migrating vapor and shuts off part of the condenser to condensation.

In non-VCHP heat pipes, an increase in the heat load at the evaporator can cause a dramatic temperature increase in the working substance. In VCHP pipes, however, fluctuations in heat load have a much smaller effect on the working substance temperature. In the case of a heat load surge in a VCHP, for instance, the increased system pressure will compress the inert gas plug and expose more pipe length to

condensing vapor. Since there is an increase in the interfacial area between the working substance and the heat sink, there is less upward pressure on the temperature. Thus, the temperature increase caused by the increase in heat load is mitigated.

In the case of a sudden drop in heat load in a VCHP pipe, the lower system pressure will allow the inert gas plug to expand and choke off the available area for condensing vapor. Thus, the temperature decrease will be mitigated. In either case, the presence of the inert gas serves to buffer the effects of heat load fluctuations. Figures 2.3 and 2.4 illustrate the use of inert gases in VCHP.

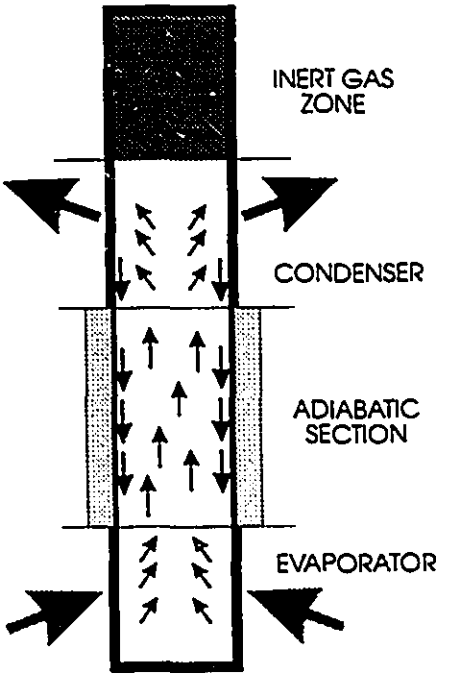

Figure 2.3
4 Zone Thermosyphon

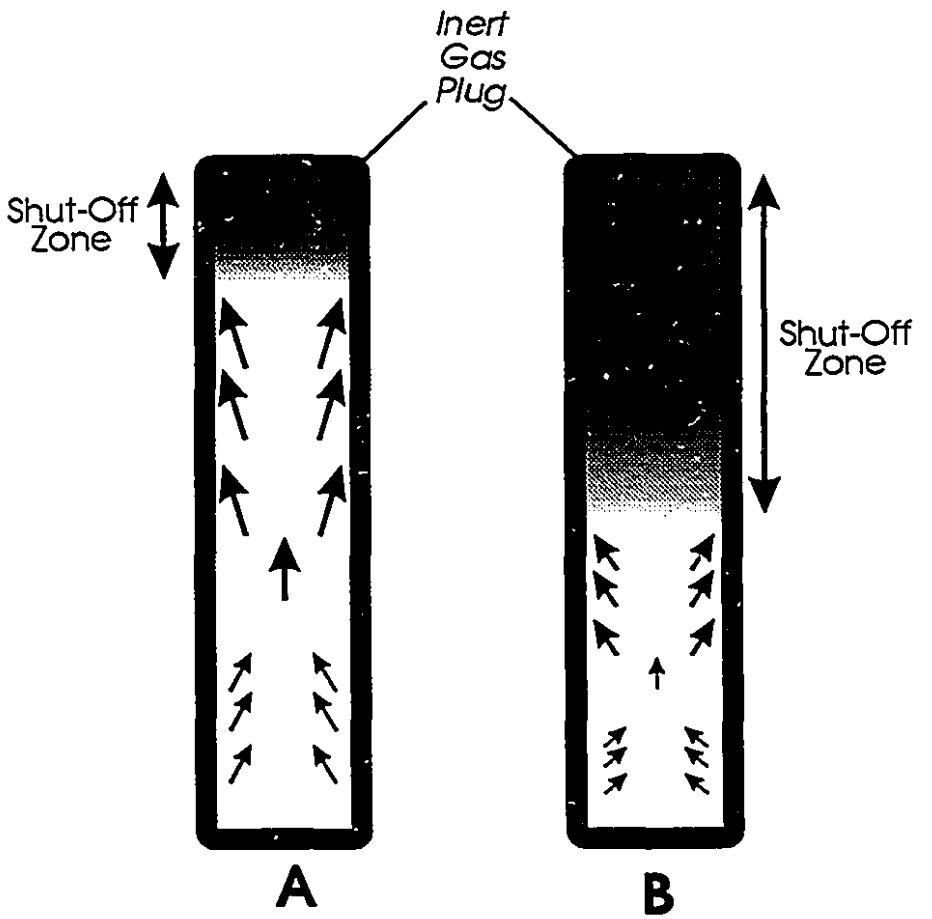

Figure 2.4
Shut-off Zone in a Thermosyphon under High Heat Load (A) and Low Heat Load (B)

2.4 Applications

Heat pipes, in their simplest form, have been used long before Gaugler's famous 1942 patent application[ix]. Angier March Perkins' "ever full" water boiler[x] (Figure 2.5) of the late 19th century was based on what would now be known as a gravity heat pipe.

Perkins, very possibly the original inventor of the heat pipe concept, correctly anticipated many of the uses for heat pipes : Heat exchangers[xi] , waste heat recovery[xii] and cooling.[xiii]

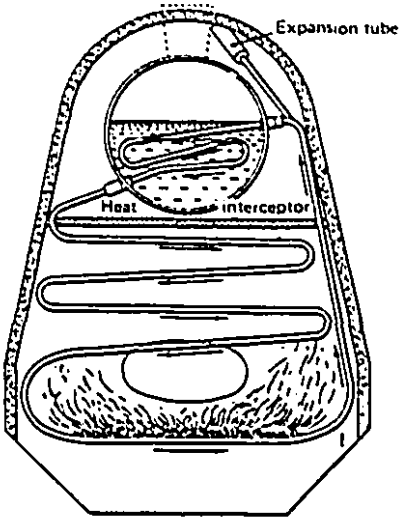

Figure 2.5
Perkins Boiler

The heat pipe did not obtain it's name until the term was coined by M. Grover in 1964[xiv]. In 1967, the first satellite heat pipe test was conducted[xv], breaking ground in what remains the single most important heat pipe application. By 1968, 80[xvi] scientific papers had been published on the subject of heat pipes, including those dealing with novel application in the fields of air conditioning, engine cooling and the temperature control of electronic components.[xvii ,xviii ,xix] From the 1970's to the present day, thousands of scientific papers have been published on many aspects of heat pipe applications and theory.

2.4.1 Heat Pipe Applications in Metallurgy

While heat pipes have been used successfully in a large variety of space and terrestrial heat transfer applications, there are, as yet, relatively few metallurgical processes which take advantage of the heat pipe's enormous capacity for heat removal.

For the metallurgical industry, the potential advantages of implementing heat pipe technology are enormous. The extremely high heat transfer rates allow the heat pipe shell, including the evaporator, to operate at temperatures much lower than that of the heat source[xx]. This can be of large advantage in many pyrometallurgical operations, and in particular, in furnaces and converters where apparatus must endure severe thermal convective environments.

2.4.1.1 Work Conducted Outside McGill

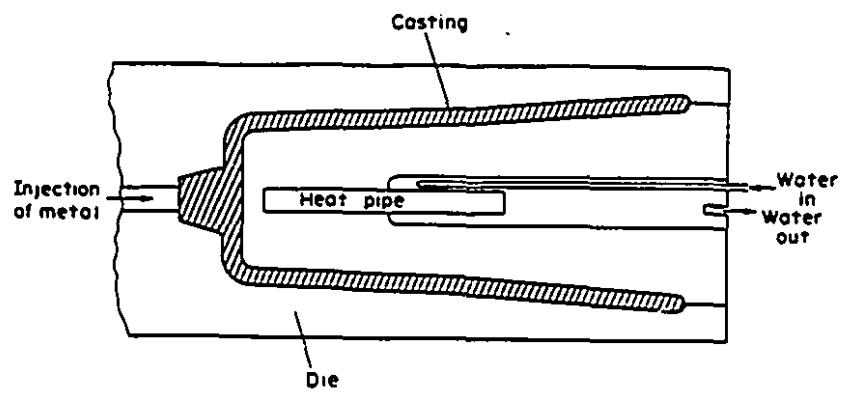

Figure 2.6
The Heat Pipe Used to Supplement Cooling in a Die. ***(Dunn, P. 239)***

Outside of the work conducted at McGill University, the majority of published papers dealing with heat pipe applications in metallurgy concern improving existing water-cooling technology in dies and moulds. Heat pipes have been used to mitigate temperature gradients within the die as well as removing heat from hot spots within the assembly. Figure 2.6 illustrates a simple, typical usage of heat pipes within a die assembly.

Other notable applications of heat pipe technology in the field of process metallurgy include the use of heat pipes as an alternative to water in the cooling shanks of graphite arc furnace electrodes[xxi] and the use of annular heat pipe sections as isothermal furnace liners[xxii].

- 2.4.1.2 Continuous Measurement of Melt Temperature

The continuous measurement of melt temperature using a heat pipe-sheathed thermocouple is a heat pipe application developed at McGill University by Choi and Mucciardi[xxiii].

In modern steelmaking processes, avoiding problems such as breakouts or tundish freeze-up often require knowledge of the instantaneous steel temperature in the tundish. Unfortunately, continuous temperature measurement of molten steel is not always feasible with current technology. One of the major problems is that the conventional thermocouples employed to measure temperature in the steel cannot withstand the severe corrosion around the slag line. This sensitivity requires that the thermocouples be inserted into a protective refractory sleeve. Because of chemical

attack from the slag, current sleeves have a lifespan of less than 10 hours, after which time the entire assembly, including the refractory sleeve, must be replaced.

A novel innovation has been developed whereby the thermocouple is protected by an annular heat pipe sleeve at the slag line. Figure 2.7 illustrates this innovation.

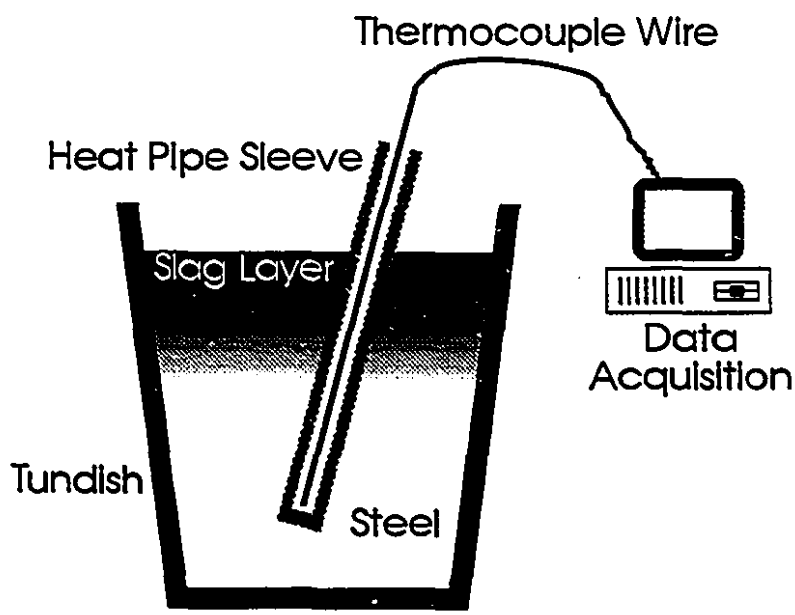

Figure 2.7
Measurement of Steel Temperature with a Heat Pipe-Sheathed Thermocouple

The ability of the heat pipe to evacuate large quantities of heat causes solid accretions to form on the walls of the pipe, thus producing a protective barrier against further chemical attack from the slag. Using this process, the thermocouple wire is protected indefinitely and continuous measurement of steel temperature is possible.

- 2.4.1.3 Liquid Aluminum Probe.

This is another metallurgical heat pipe application pioneered at McGill. Meratian et al. have developed an innovative method by which cooling-curve data for liquid aluminum melts may be generated on a semi-continuous basis.[xxiv,xxv]

For batches of liquid aluminum prepared at foundries, melt composition may be determined by means of producing a *cooling curve*, a technique commonly referred to as *thermal analysis*.[xxvi] The location of the solidus and liquidus temperatures, coupled with the overall shape of the curve provide a cooling curve "signature" which is characteristic of a given alloy composition. Figure 2.8 illustrates cooling curves for two different batches of 356 alloy ingot.

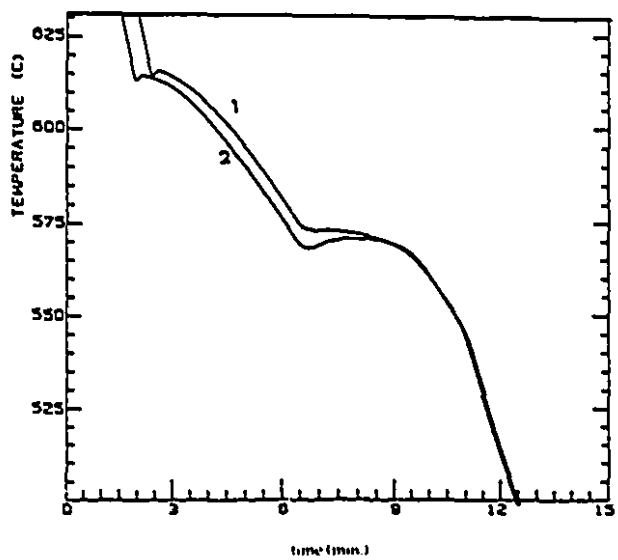

Figure 2.8
Cooling Curves Obtained from Two Batches of 356 Alloy Ingot

The traditional batch method of generating cooling curves involves removing a sample of metal from the melt and then cooling it in a crucible while monitoring the temperature change with a thermocouple. This is a ponderous process which is quite difficult to automate.

The heat pipe aluminum probe, however, is semi-continuous, and is highly suitable for automated data acquisition.

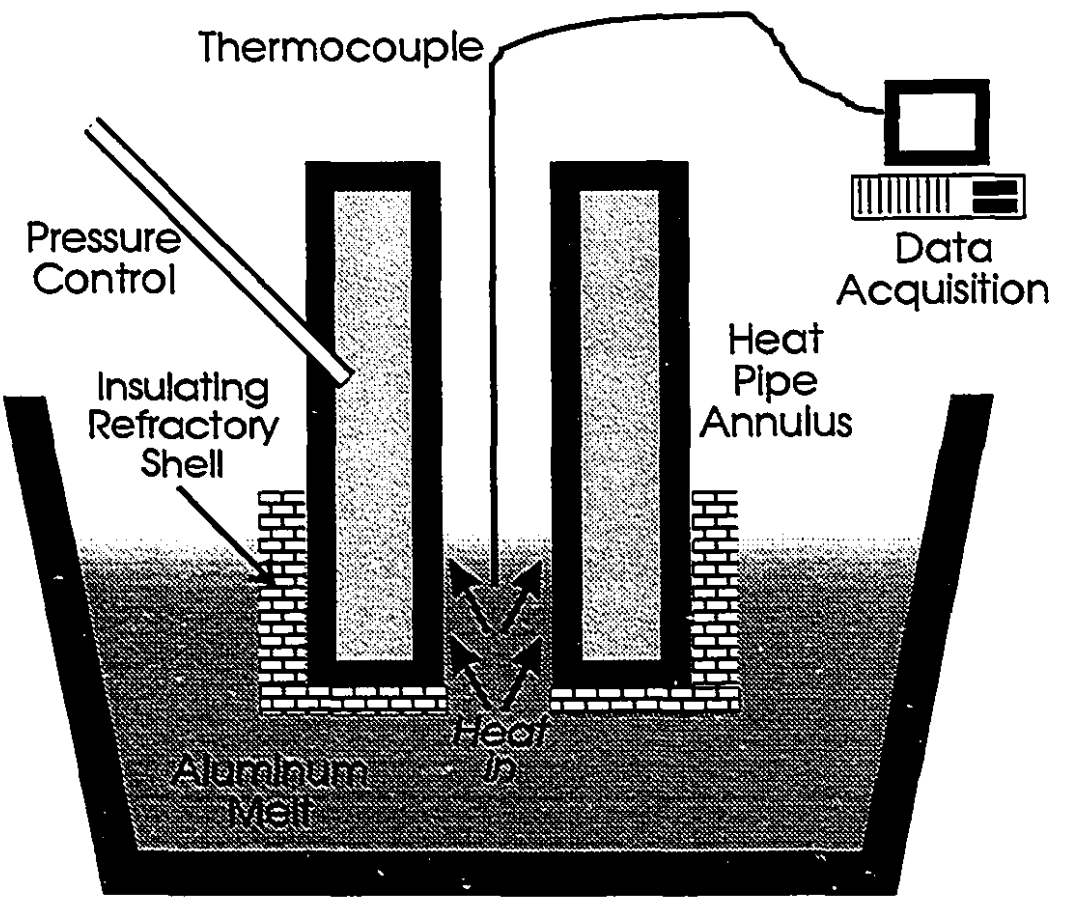

Figure 2.9
Cross-Section Schematic of Heat Pipe Aluminum Probe

As with the thermocouple sheath heat pipe, the working substance in the aluminum probe heat pipe shell is contained within a steel annulus. The central core at the bottom of the pipe is used to trap a relatively small aluminum pellet for analysis.

When the heat pipe chamber is depressurized, the working substance temperature decreases and heat is absorbed from the melt trapped in the core section (see Figure 2.9). The cooling curve for this trapped sample is recorded by means of a thermocouple attached to a data acquisition system. Once the cooling curve has been generated, the heat pipe outer annulus is pressurized, the working substance heats up and the sample is remelted. Another cycle is ready to begin.

• 2.4.1.4 Top Blowing Lances for Mitsubishi Copper Production Process

The Mitsubishi process is the only known process for copper production which is truly continuous. Matte conversion is done continuously, as opposed to the batch-type process used with Peirce-Smith converters.[xxvii] The distinguishing elements of the Mitsubishi process are as follows (Botos, p.11) :

1) Smelting and converting reactions take place in separate furnaces.

2) Transportation of melt is carried out through launders connecting the furnaces.

3) Top blowing lances are used for air blowing and solid materials feeding.

Figure 2.10 provides an overview of the Mitsubishi process.

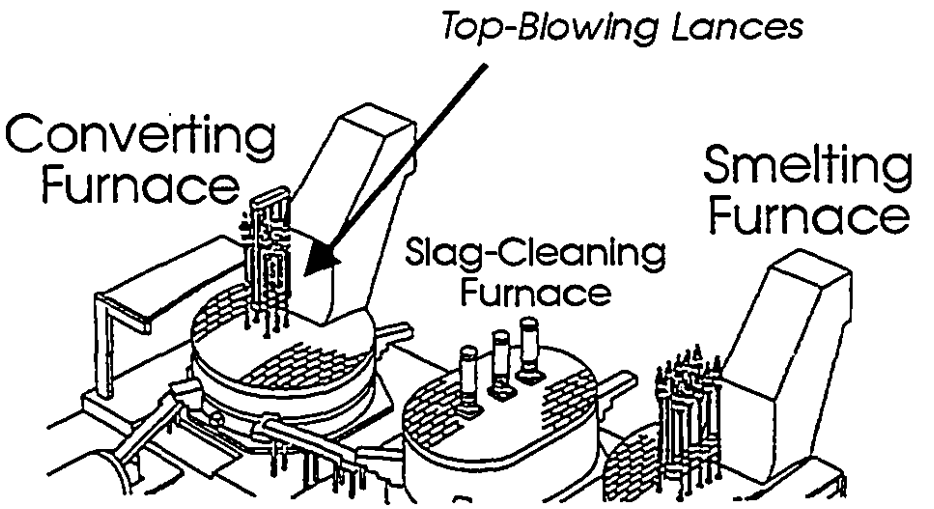

Figure 2.10
The Mitsubishi Process for Copper Production

One of the main difficulties with the Mitsubishi process is that the top-blowing lances which are fundamental to the process[xxviii] dissolve continuously during the blow due to a combination of high temperatures, chemical attack and dissolution by matte and blister copper. This results in a substantial materials cost, since the high chromium stainless steel lances are expensive to replace.

Another serious problem involves the positioning of the lance tip within the furnace. Under ideal conditions, the lance tip is situated 0.5 m from the bath surface (Botos, p.15). Given that the lance is continuously dissolving, the exact position of the lance tip within the furnace is not known with certainty during the blow. This means that it is impossible to optimize the process.

These problems motivated the development of the heat pipe injection lance[xxix] for testing at the Kidd Creek copper production facility. The heat pipe injection lance

was first tested at Kidd Creek on August 13, 1991 and successfully resisted failure for a period of 2 days. The success of this and subsequent tests suggests that heat pipe injection lances will soon have a prominent role in installations employing the Mitsubishi process. Figures 2.11 and 2.12 schematize the role of a heat pipe top-blowing injection lance.

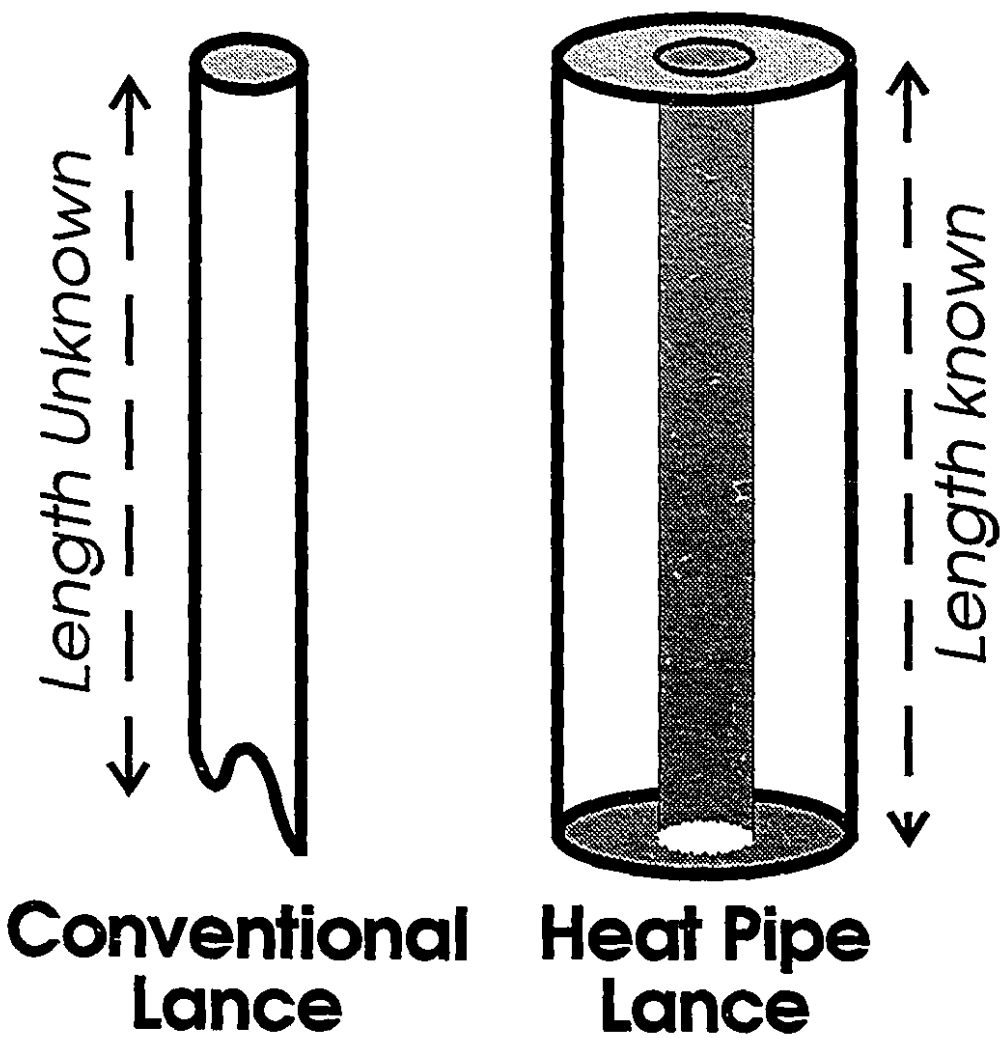

Figure 2.11
Heat Pipe Injection Lance vs. Normal Injection Lance

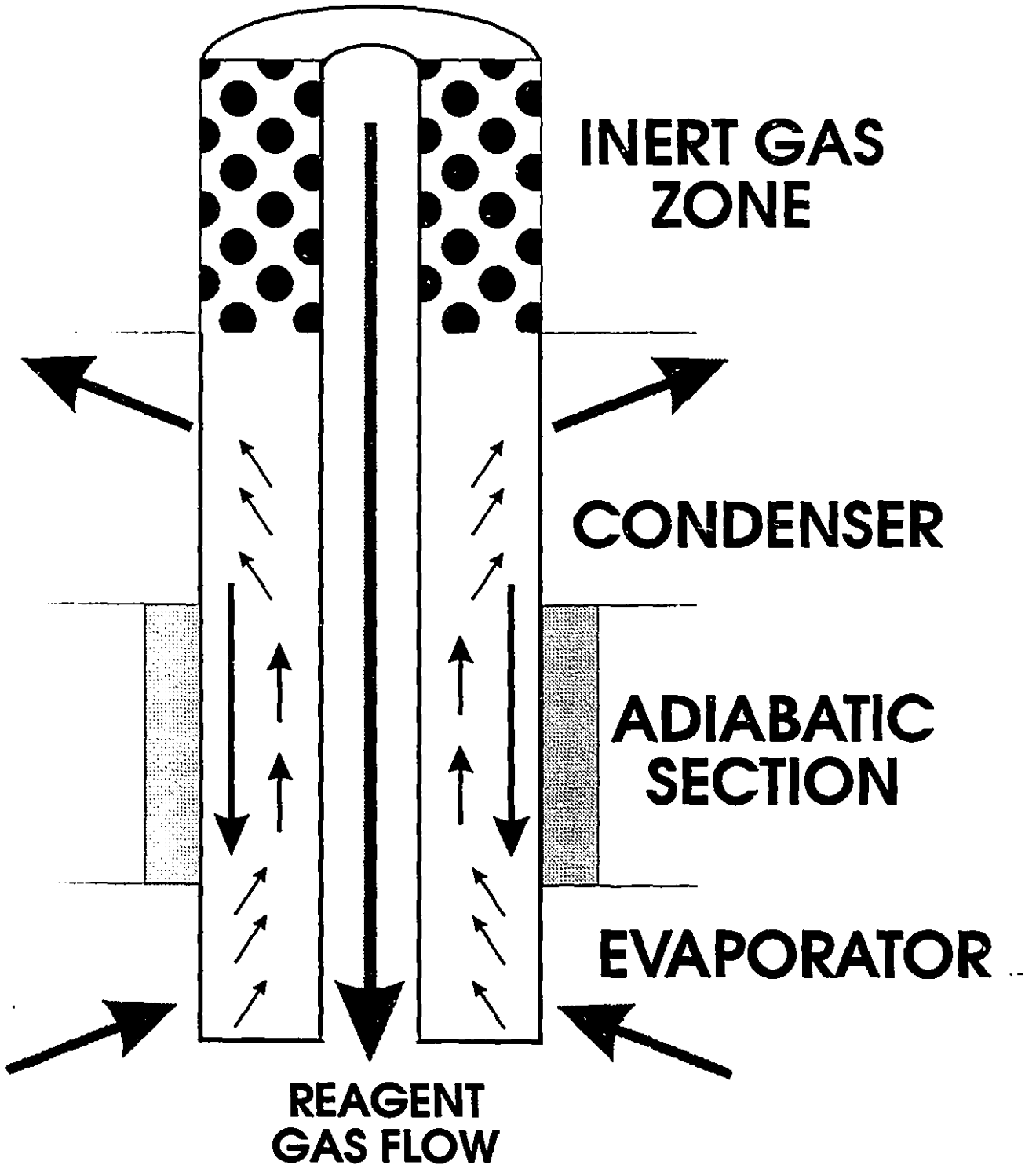

Figure 2.12
Schematic of a 4-Zone Annular Heat Pipe Injection Lance

- 2.4.1.5 The BOF Steelmaking Lance

Of the top lances used with-bath smelting processes, the most prominent is the BOF oxygen lance which is used to inject pure oxygen into a pig iron melt. The vast majority of integrated steelmaking concerns now use this process to produce steel. Because of the extreme temperatures encountered in oxygen steelmaking, it is necessary to cool the BOF lance with a relatively large quantity of water that is pumped within a cooling jacket.

Recent innovations by Mucciardi et al. of the McGill Department of Metallurgical Engineering have demonstrated a viable alternative to the water-cooled BOF injection lance.

> "...A laboratory scale, oxygen top blowing, injection lance for BOF steelmaking has been developed and tested. This novel lance, based on heat pipe technology, can be operated without any cooling circuit whatsoever. Heat fluxes of about 1 MW/m^2 at the lance tip are readily dissipated even with the lance operating at typical industrial rates of decarburization and oxygen utilization..." [xxx]

The heat pipe BOF steelmaking lance works in much the same fashion as the lances designed and tested for the Mitsubishi copper production process. As yet, heat pipe BOF lances have only been tested in laboratory-scale steelmaking experiments. These experiments have yielded excellent results and indicate that BOF steelmaking lances have the potential to become an important heat pipe application in metallurgy. A photograph of an experimental heat pipe BOF steelmaking lance is shown in Figure 2.13.

Figure 2.13
Photo of Experimental Heat Pipe BOF Steelmaking Lance

- 2.4.1.6 Heat Pipe Cooling Rolls

Following the continuous casting of steel, the rolled sheet[xxxi] is typically cooled with a series of water sprays. A project has been initiated at McGill University by Frank Mucciardi and Ning Jin to apply heat pipe cooling rolls to the task of cooling the metal sheet.[xxxii]

By using heat pipe rolls, heat can be extracted from the 'evaporator' (the angular segment of the roll which is in contact with the metal at a given instant) and used to

vaporize the thin working substance film which coats the inner wall of the hollow heat pipe roll. The vapor condenses on the 'condenser' area (the angular segment which is not in contact with the metal). Heat removal rates could be increased by blowing air or water through a parallel pipe network running axially within the core of the roll. Figure 2.14 illustrates how heat pipe rolls might be used to cool steel sheet.

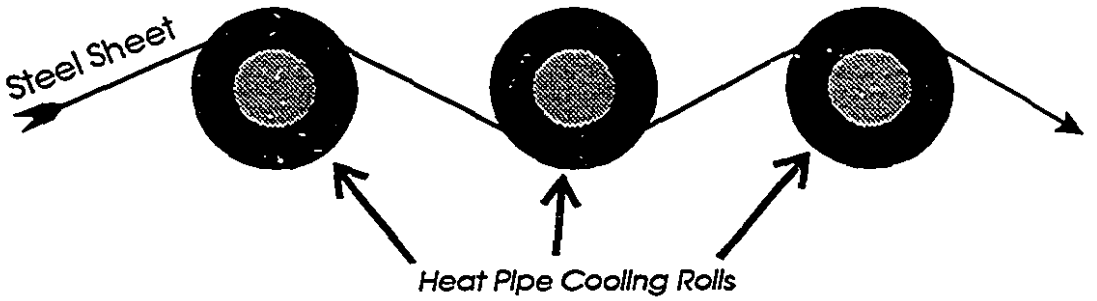

Figure 2.14
Heat Pipe Rolls

While this project is still in its preliminary stages, initial design projections are very encouraging.

3

Heat Pipe Operation

3.1 Working Substance

3.1.1 Chemical Compatibility

Chemical compatibility between working substance and pipe shell is necessary for heat pipe longevity. Certain combinations have been found to be excellent, such as copper/water or Pyrex/freon. A copper/water heat pipe operating at 120° C for 135,000 hours[xxxiii], for instance, established what is thought to be the current world record for operating longevity (Dunn, p.56). On the other hand, certain combinations have been found to be reactive. In an aluminum/water pipe, for example, the water will oxidize the aluminum and produce hydrogen gas. The H_2 gas, which is inert, will rapidly accumulate and completely plug the condenser[xxxiv]. Sodium, potassium and cesium, popular choices for high-temperature applications, are compatible with stainless steels (Silverstein, p.57) and other modified steels.

3.1.2 Thermal Stability

Experiments conducted at McGill by Meratian et al. have shown that alloy constituents can be eliminated selectively from the active working substance pool by means of solid-phase precipitation and escape to the pressure control line.[xxxv] This produces the undesirable result that the composition of the working substance pool will progressively degrade over time. Utmost care must be taken in the use of metal alloy working substances and organic fluids (Dunn, p.91) to ensure that this phenomenon does not, eventually, corrupt the function of the working substance.

3.1.3 Condensate

3.1.3.1 Wettability

For the condensate return, it is desirable that the liquid wet the pipe and travel as a stable film which has approximately constant thickness over a given pipe section. If this is not the case, then the condensate may be shunted into rivulets. In the evaporator, above the liquid pool, certain wall sections will be 'dry' and hot spots will be produced. These areas of heat concentration can lead to pipe failure. This illustrates the desirability of a pipe-wetting working substance.

The condition for wetting to occur between a given liquid and a given surface is the following: That the total surface energy is at a minimum when the angle of contact between the liquid droplet and the surface is less than 90 degrees. Figure 3.1 illustrates the conditions of wetting and non-wetting.

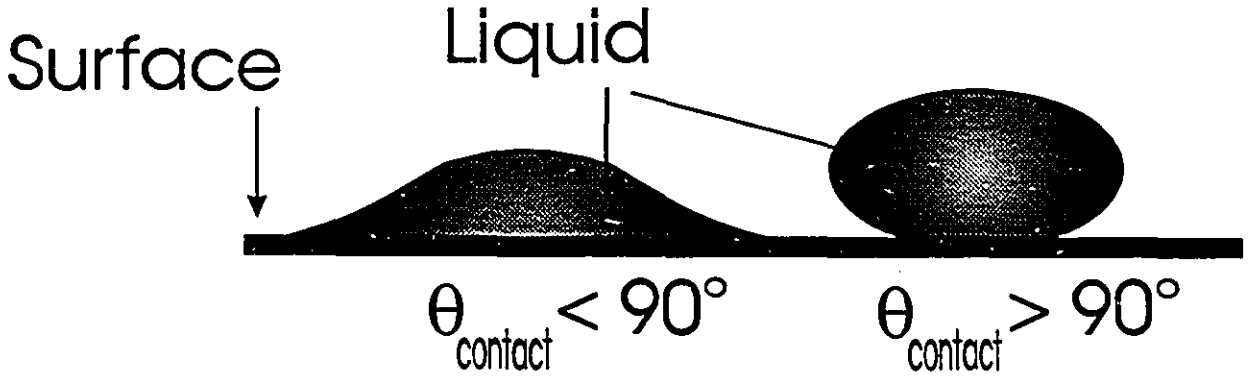

Figure 3.1
Wetting (Left) and Non-Wetting (Right) of a Surface

- 3.1.3.2 Flooding Limit and Entrainment Limit

Condensate return to the evaporator may also become unstable if the interaction between the counter current liquid/vapor flow and the viscous shear forces occurring at the liquid/vapor interface inhibit the return of liquid to the evaporator.

> "... When this occurs, the heat pipe is said to have reached the *flooding limit*. Further increases in the heat input result in increased vapor velocities, which may cause the liquid flow to become unstable. In the most severe cases, waves may form and the interfacial shear forces may become greater than the liquid surface-tension forces, resulting in liquid droplets being picked up or entrained in the vapor flow and carried to the condenser. This entrainment of liquid droplets can limit the axial flux and is referred to as the *entrainment limit*... Although both flooding and entrainment result in excess liquid accumulation in the condenser and dry-out of the evaporator..., they can be differentiated by the presence of liquid droplets entrained in the vapor stream..." [xxxvi]

Various authors have presented mathematical correlations for predicting the onset of flooding and/or entrainment in thermosyphons as a function of the

thermodynamic and fluid properties of the working substance. Peterson and Bage have examined 16 different mathematical correlations of this type. Unfortunately, they report that the studied correlations yield variations spanning a geometric factor of five (p.152).

3.1.4 Temperature Range

While, theoretically, a heat pipe may be operated at virtually any internal pressure, it is generally desirable for the system pressure to be at or below atmospheric. This stipulation, in turn, prescribes the allowable temperature range for any given pure working substance since the vapor pressure and temperature for a pure substance are coupled by the well-known Clausius-Clapeyron equation :

$$\ln\left(\frac{P_{ws}}{101300}\right) = \frac{a}{T_{ws}} + b \qquad \text{Eq. 3.1}$$

Figure 3.2 illustrates the operating temperature range for various heat pipe fluids. The temperature range calculated corresponds to the pressure range of 6895 Pa to 689 500 Pa.

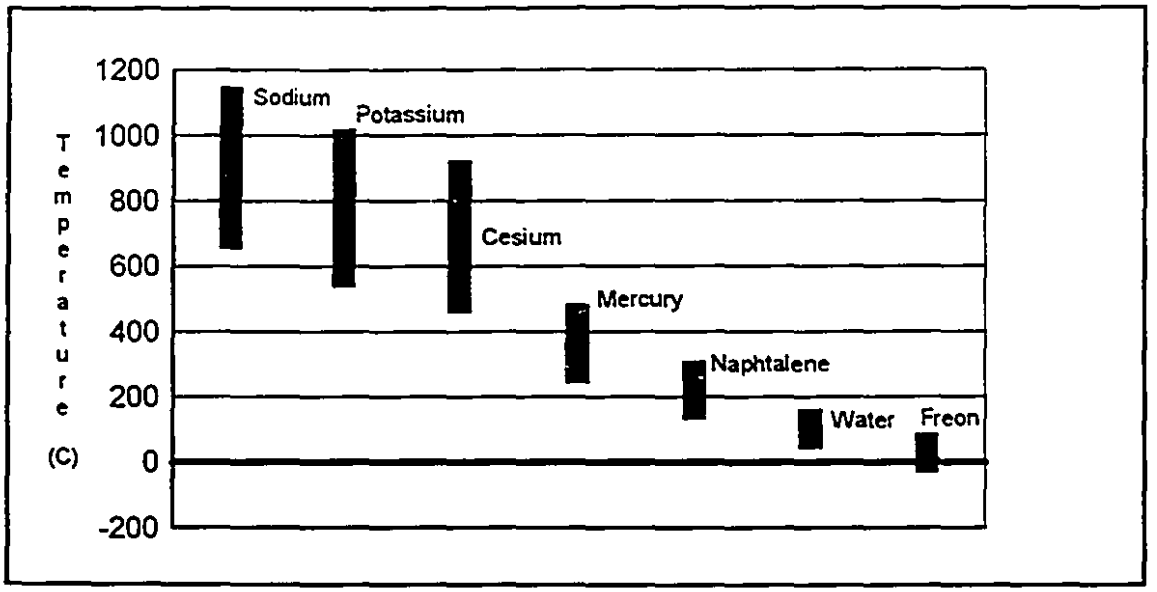

Figure 3.2
Operating Range for Seven Working Substances

3.1.5 Working Substance Heat Transport Capability

Just as important as the temperature range, however, is the *Liquid Heat Transfer Parameter* (Silverstein, p.54) also known as the Merit number (Dunn, p.24). This index, defined in equation 3.2, may be used to determine the heat transport capability of a given working substance.

$$P_{ht} = \frac{\rho_l \cdot \sigma \cdot \kappa}{\mu_l} \qquad \text{Eq. 3.2}$$

P_{ht} is a positive function of density, latent heat of evaporation and surface tension. As one might expect, it varies inversely with liquid viscosity.

3.1.6 The Boiling Limit

Boiling occurs when fluid is evaporated to the gas phase at a solid-liquid interface. The vapor originates as bubbles which form at the heating surface. The phenomenon is complex to analyze because the heat and mass transfer is partially governed by the growth and movement of these bubbles as they rise to the liquid surface. The vapor bubble dynamics is, in turn, a function of temperature differential, surface microstructure, fluid thermophysical properties, the fluid flow regime and other parameters.

Figure 3.3 illustrates the different regimes of boiling[xxxvii]. The highest boiling heat transfer coefficients are yielded under the nucleate boiling regime wherein bubbles begin to form on the heated surface, travel through the liquid and are subsequently dissipated at the surface of the liquid. With increasing heat differential, however, bubbles are formed so rapidly that they completely blanket the heating surface and prevent the inflow of fresh liquid. The bubbles then coalesce into a vapor film which coats the heating surface. Heat must now be conducted through this gas film and the heat flux is reduced. The onset of this gas film phenomenon is termed the *critical heat flux*. $q''_{crit,b}$ is generally on the order of 10^6 W/m^2 [xxxviii]. This maximum heat flux is often referred to as the *burnout point* or the *boiling crisis* or, in the case of heat pipes, the *boiling limit*.

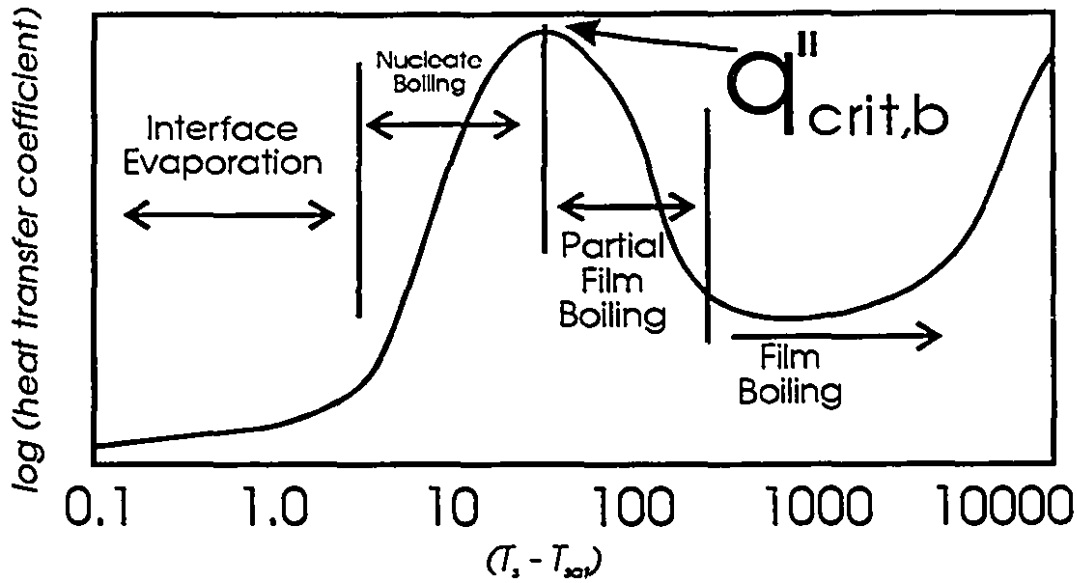

Figure 3.3
Heat-Flux Data from an Electrically Heated Platinum Wire

$q''_{crit,b}$ for a given substance has been estimated by Zuber[xxxix] based on the stability requirements of the interface between the vapor film and the liquid. See equation 3.3.

$$q''_{crit,b} = \frac{\pi}{24} \cdot \kappa \cdot \rho_v \cdot \left(\frac{\sigma \cdot g \cdot g_c \cdot (\rho_l - \rho_v)}{\rho_v^2}\right)^{1/4} \cdot \left(\frac{\rho_l + \rho_v}{\rho_l}\right)^{1/2} \qquad \text{Eq. 3.3}$$

• 3.1.7 Diffusion Freeze-Out

When the heat sink temperature is below the freezing point of the working substance (as is often the case with liquid metal heat pipes), working substance vapor which diffuses into the inert gas zone may freeze on the pipe walls, thus depleting the

available inventory of working substance. If the process continues unabated and sufficient quantities of the working fluid are permitted to solidify in the inert gas zone, the pipe will cease functioning due to *diffusion freeze-out*. This phenomenon has been studied extensively by Edwards, et al.[xi].

3.2 Heat Pipe Shell

3.2.1 The Sonic Limit

As the heat load on a thermosyphon increases, so does the vapor flow from the evaporator to condenser. Under extreme heat load, vapor velocities may become extremely high, particularly at the mouth of the evaporator, where mass flow is highest. The *sonic limit* is encountered when the migrating vapor in a heat pipe attains sonic speeds. When the sonic limit is encountered, the application of additional heat load fails to increase the mass flow of vapor. Instead, the evaporator temperature increases unabated, and large axial heat gradients develop in the working substance.

Dunn (p.73) reports the sonic limit as follows :

$$Q_{tot} = A_{cs} \cdot 0.474 \cdot \kappa \cdot \left(\rho_v \cdot P \right)^{1.5} \qquad \text{Eq. 3.4}$$

A heat pipe must have sufficient cross-sectional area to accommodate the vapor flow which results from the applied heat load.

3.2.2 Fluid Inventory

Fluid inventory in a pipe must be sufficient to wet all internal surfaces during pipe operation. If the liquid reservoir at the evaporator is too large, however, the flow of vapor bubbles from the evaporator wall surface will be hampered by the hydrostatic head pressure of the pool. This pressure differential will give rise to an axial temperature gradient. Strel'tsov[xli] has proposed an equation which yields the optimum fluid inventory for a thermosyphon:

$$G = \left(0.8 \cdot l_c + l_a + 0.8 \cdot l_e\right) \cdot \left[\frac{3 \cdot q_{tot} \cdot \rho_l \cdot \pi^2 \cdot r_i^2}{\kappa \cdot g}\right]^{1/3} \qquad \text{Eq 3.5}$$

3.3 Boundary Conditions

3.3.1 Evaporation of the Working Substance

If the boiling limit is respected, the heat transfer regime in the evaporator will be one of nucleate boiling. The turbulent mixing in the liquid film which is caused by bubble growth and detachment gives rise to very high heat transfer coefficients. Boiling heat transfer rates in the nucleate boiling regime may be estimated using the Rohsenow correlation[xlii] :

$$q'' = \mu \cdot \kappa \cdot \left[\frac{g(\rho_l - \rho_v)}{g_c \cdot \sigma} \right]^{1/2} \cdot \left[\frac{C_p \cdot (T_s - T_{sat})}{C_{sf} \cdot \kappa \cdot \mathrm{Pr}_{sat}} \right]^3 \qquad \text{Eq. 3.6}$$

Despite the non-linear dependence of heat flux on temperature difference, it is nevertheless quite common to approximate the non-linear relationship with a linear expression of the following form :

$$q'' = h_b \cdot (T_s - T_{sat}) \qquad \text{Eq. 3.7}$$

3.3.2 Condensation of the Working Substance

The amount of heat rejected to the condenser is equal to the mass of vapor which condenses multiplied by the working substance's latent heat of vaporization. If the liquid wets the surface of the heat pipe, the condensation regime is known as *film condensation*. Otherwise, the process is called *dropwise condensation*[xliii].

Under the film-condensation regime, the pipe surface is blanketed by the condensate film, which grows in thickness as it moves down towards the evaporator. Heat transfer through the film is driven by the difference between the vapor saturation and wall surface temperatures. The film condensation process, as schematized with the incorporation of Nusselt's modeling assumptions[xliv] is illustrated in Figure 3.4,

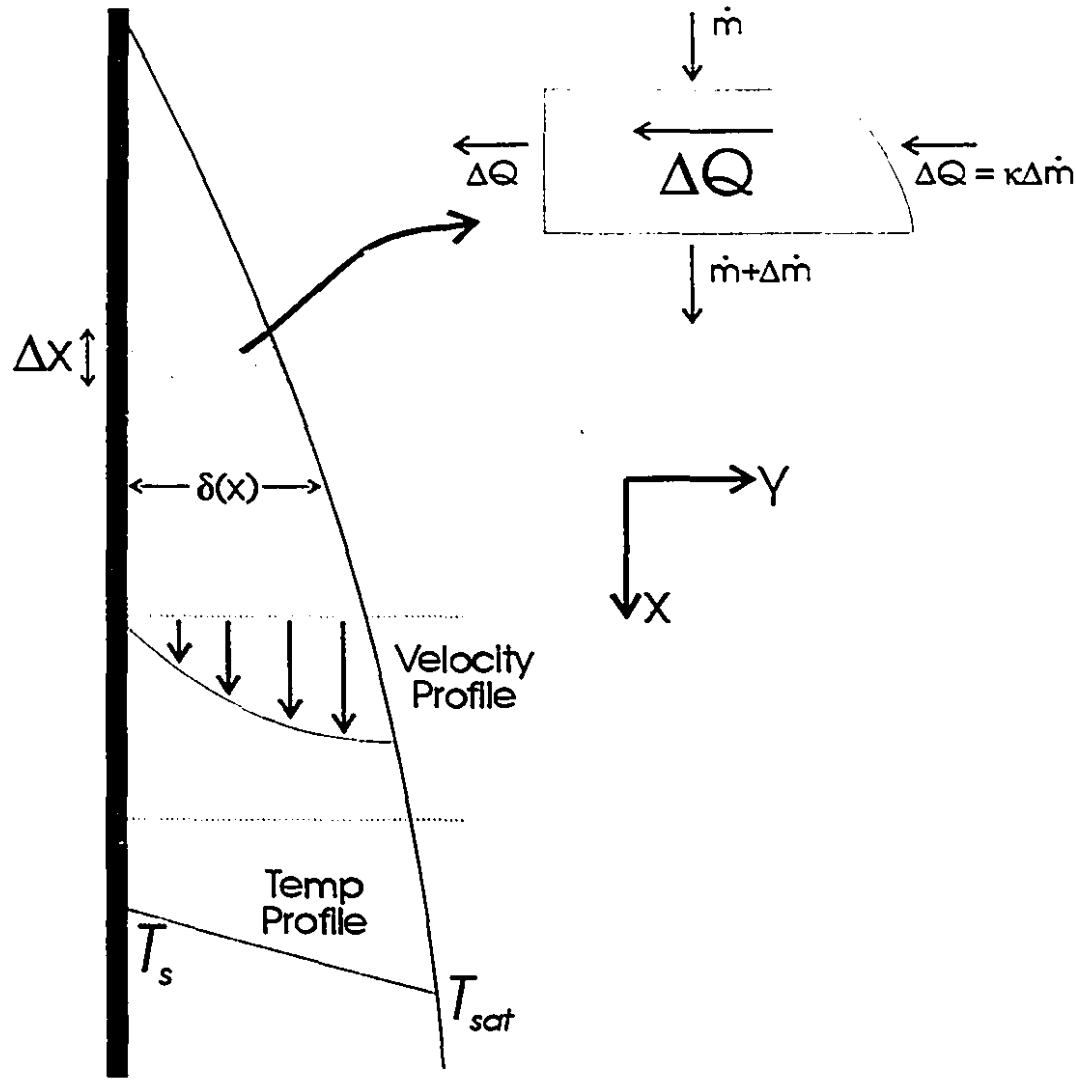

Figure 3.4
Nusselt's Analysis of Laminar Film Condensation on a Vertical Surface

Nusselt's analysis is conducted under the assumption of laminar flow, constant property fluid, pure vapor at its saturation temperature, negligible shear force at the liquid-vapor interface, negligible momentum and energy transfer by convection in the condensate film in addition to Prandtl's standard boundary layer approximations. Because the film thickens with distance, the local heat transfer coefficient will *decrease*

with distance. Thus, the mean heat transfer coefficient for a given segment will be a diminishing function of length. Equation 3.8 presents Nusselt's computed heat transfer coefficient for film condensation on a vertical surface.

$$\bar{h}_{av} = 0.943 \cdot \left[\frac{g \cdot \rho_l \cdot (\rho_l - \rho_v) \cdot k_l^{\,3} \cdot \kappa}{4 \cdot \mu_l \cdot (T_{sat} - T_s) \cdot l_c} \right]^{1/4} \qquad \text{Eq. 3.8}$$

3.3.3 Cooling of the Condenser

At the external wall of the outer pipe shell, the summation of the convective and radiative heat fluxes yields the total cooling of the pipe. Radiation is generally the primary mechanism for the cooling of high temperature liquid metal heat pipes. In low temperature pipes, or high temperature pipes with water cooling jackets, convection is generally the dominant heat transfer mechanism.

3.3.3.1 Radiation

The quantity of radiative heat which a body exchanges with the outside environment is governed by the Stefan-Boltzmann law of thermal radiation, illustrated in equation 3.9.

$$q''_{rad} = \varepsilon \cdot \beta \cdot F \cdot \left(T_s^{\,4} - T_{env}^{\,4} \right) \qquad \text{Eq. 3.9}$$

- 3.3.3.2 Convection

In the case where natural convection cools the condenser section, the following relation for vertical walls (Holman, p. 343) may be used.

$$h_{con} = .10 \cdot \frac{k_f}{l_c} \cdot \left[\frac{g \cdot \mathrm{B}_f \cdot \left(T_s - T_{env}\right) \cdot l_c^{\,3} \cdot C_{p,f} \cdot \mu_f}{{\nu_f}^2 \cdot k_f} \right]^{1/3} \qquad \text{Eq. 3.10}$$

The subscript, *f*, describes the various fluid properties as being *film properties*. These properties are evaluated at the film temperature, which is often estimated as ½ (T_s-T_{env}).

3.3.4 The Reagent Gas

While natural convection and radiation typically cool the external shell, heat may also be released by means of working substance condensation on the outer wall of the inner pipe, as illustrated in Figure 3.5, below. The reagent gas which flows through the inner pipe will increase in temperature as it absorbs heat from the inner pipe wall. In this manner, the reagent gas can obtain substantial preheat. A control volume energy formulation for the gas flow is illustrated in Equation 3.11 and Figure 3.6. Turbulent dissipation is neglected.

$$\rho_r \cdot v_g \cdot C_{p,gas} \cdot \frac{dT_{gas}}{dZ} + v_g \cdot A_g \cdot \frac{dP_{gas}}{dZ} = q'' \cdot 2\pi \cdot r_b \cdot dZ \qquad \text{Eq. 3.11}$$

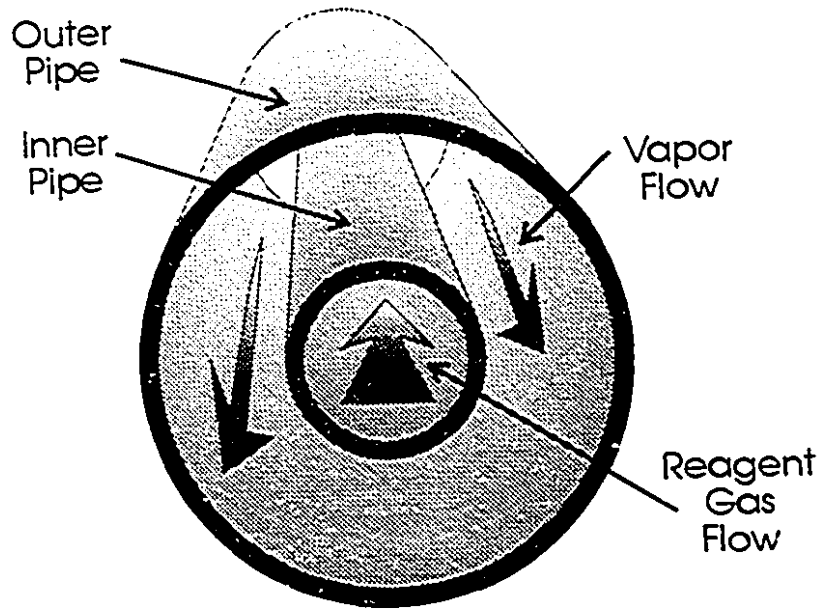

Figure 3.5
Cross-Section of Thermosyphon Injection Lance at Condenser

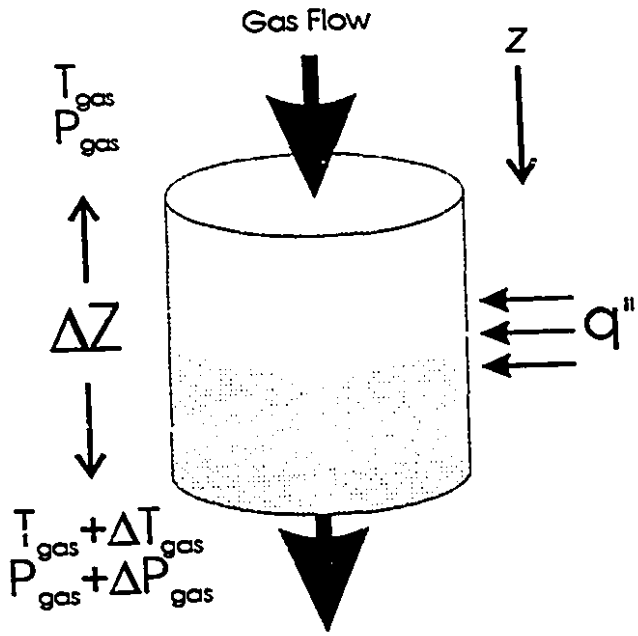

Figure 3.6
Energy Balance on a Segment of Gas Flow

4

Modeling

4.1 Aspects of Heat Pipe Modeling

Because thermosyphons lack a wick structure, many aspects of their modeling are relatively straightforward. In variable conductance thermosyphons, however, difficulties arise concerning treatment of the interfacial layer between the convecting vapor and the stagnant inert gas.

> "...Temperature and concentration gradients in the region in between the gas and vapor drive the double-diffusive natural convection component. The low velocities in the diffusion region require the use of full elliptic equations, rather than the simpler parabolic forms... The greatest difficulties arise from the complicated nature of the boundary conditions. Phase equilibrium requires a highly non-linear relationship between the gas concentration and the temperature at the wall...." [xiv]

The most complex numerical models, such as that of Hijikata et al.[xvi] include diffusive transport in the interface region, wall conduction and a two-dimensional treatment of inert gas distribution. Unfortunately, the enormous complexity of full-blown 2-D models renders them mathematically time-consuming and, in the case of Hijikata et al., able to accommodate only a limited range of operating parameters.[xvii] 1-D models,

such as those of Van der Vooren[xlviii], Bobco[xlix] and Edwards et al.[l] provide more robust alternatives.

4.2 The Flat Front Model

For initial design calculations, less complexity is required. The *flat front* model proposed by Dunn (p.213) employs the following assumptions :

- Steady-state.
- Inert gas obeys the ideal gas law.
- A sharp interface exists between the gas and vapor. Gas-vapor mixing due to buoyancy effects and diffusion are ignored.
- Axial wall-conduction effects are ignored.
- Working substance is isothermal and $T_{ws} = T_{sat}$.
- Heat pipe pressure is constant. $P = P_{ws} = P_{sat} = P_{ig}$.

Previous authors have successfully employed the flat-front model at McGill to model heat pipe injection lances[li].

4.2.1 Accuracy of the Flat Front Model

For a steady-state inert-gas-loaded variable conductance thermosyphon, the inaccuracies of the flat-front model stem from the assumption of a step profile in both the axial temperature distribution and gas concentration. This is illustrated in Figure 4.1.

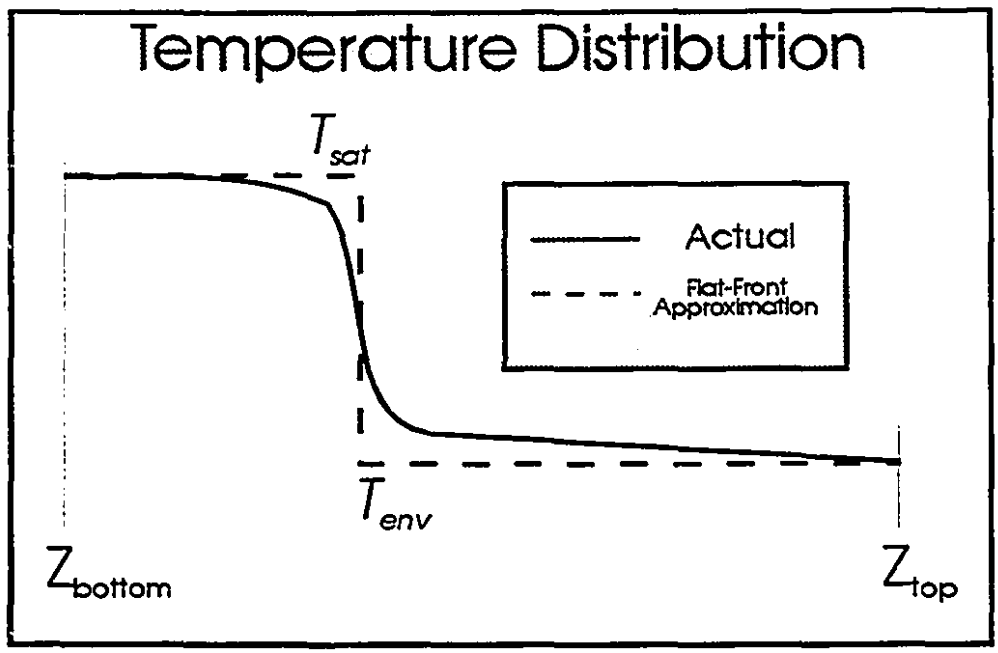

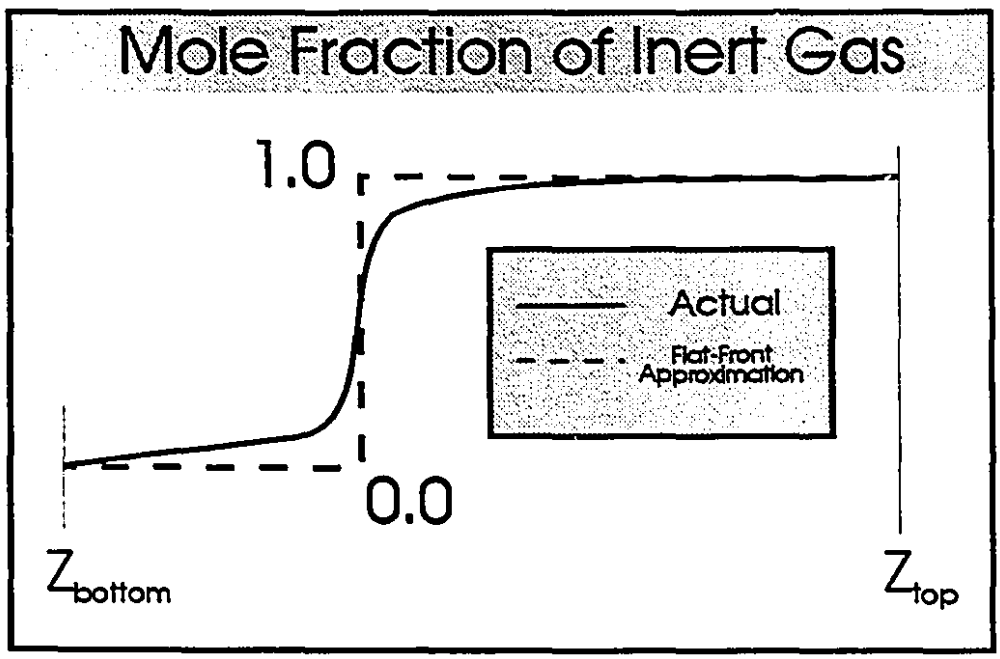

Figure 4.1
Flat-Front Approximations in the Temperature and Inert Gas Distributions

4.2.1.1 Bobco's Analysis

Bobco has performed a parametric study to determine the error incurred by adopting the flat-front model versus his own more sophisticated first-order axial model. His data[iii] illustrates that, in the case of thermosyphons without gas reservoirs, adoption of the flat-front model renders sizable errors only when the heat loads are small, as illustrated in Table 4.1

Ψ	L_c (flat front)	L_c (1st ord.)	L_c % Err.	$T_{ws,e}$ (flat front)	$T_{ws,e}$ (1st ord.)	$T_{ws,e}$ % Err.
5.55	.167	.226	26.1	44.8 °C	44.8 °C	0.00
27.8	.836	.890	6.1	51.9 °C	52.3 °C	0.77
55.6	.941	.977	3.6	77.4 °C	77.9 °C	0.65

Table 4.1
Results from Bobco's Comparison of Flat-Front Model vs. 1st Order Axial Model

4.2.1.2 Peterson's Analysis

Peterson[iii] has presented a two-dimensional diffusion model based on previous work by Hijikata, Chen and Tien (1984). Peterson's improvement consists of greatly simplifying the model and broadening its application with the inclusion of a modified integral formulation of the species equation. Peterson then performed a parametric study on the extent of the error incurred by using the flat-front model versus more complex models.

"...The relative simplicity of the integral formulation allowed this parametric study, since over 500 integral cases can be solved with the amount of computation required for one exact 2-D case..."

Figure 4.2 illustrates the extent of flat-front error in predicting the length of the shut off zone as a function of two dimensionless variables, *W* and *E*.

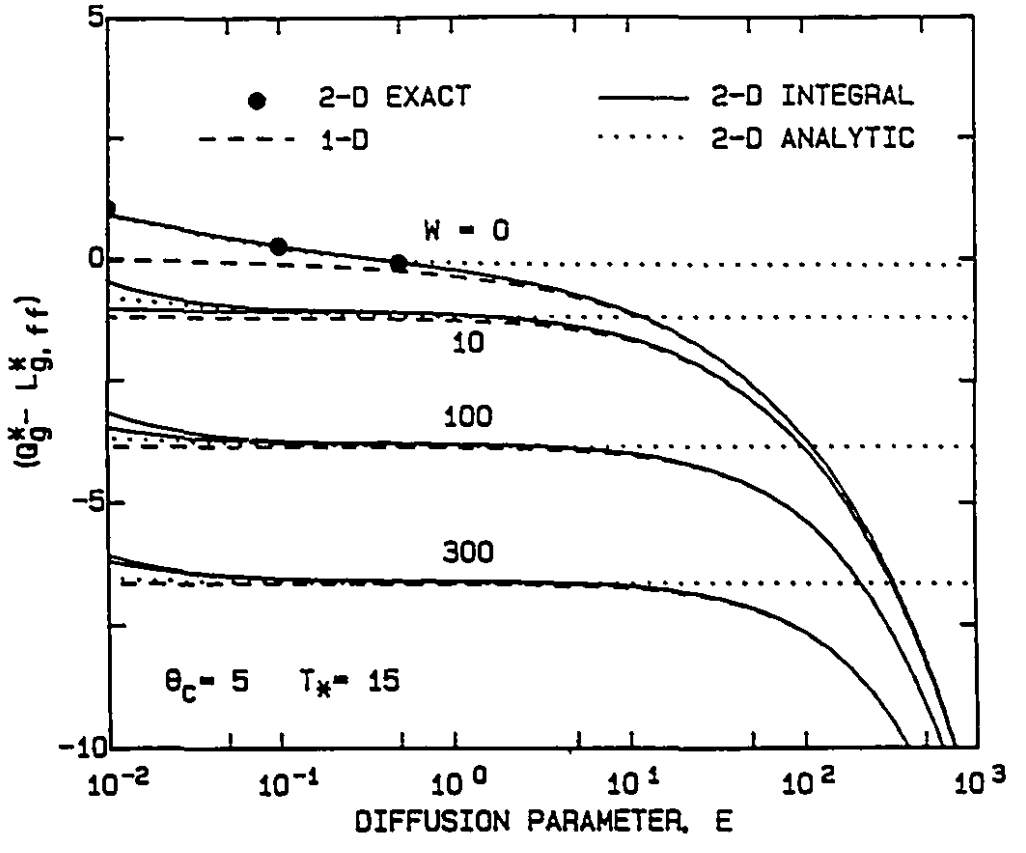

Figure 4.2
Prediction of Shut-Off Zone: Four Different Models vs. Flat-Front Model (Peterson, 1988, Fig. 2-4)

Figure 4.2 illustrates that significant errors are incurred by using the flat front model only in the case that *W* and *E* are suitably high. Also evident from the figure is the fact that 2-D effects are completely negligible at all but the smallest values of *E*.

Table 4.2 illustrates *W* and *E* values for two representative heat pipe injection lance applications.

	Botos, 1992 Mark I Injection Lance	Mucciardi, Jin and Kay, 1994 BOF Lance
Pipe Material	Stainless Steel	Stainless Steel
Working Substance	Sodium	Sodium
Pipe Length (m)	6.00	.95
Operating Pressure (kPa)	202	3
T_{ws}	1237	864
Inert Gas	Argon	Helium
C_e	1.944×10^{-2}	4.176×10^{-4}
MW_v	23	23
D	3.18×10^{-3}	2.66×10^{-3}
κ	3.6×10^{6}	3.6×10^{6}
$h_{c,tot}$	130	71.5
$(T_{sat}-T_{env})$	939	570
r_l	2.46×10^{-2}	1.12×10^{-2}
E	**1.68**	**.205**
k_s	15	15
A_k	9.45×10^{-4}	1.64×10^{-4}
W	**.89**	**3.90**

Table 4.2
Values of W and E for Two Heat Pipe Injection Lances

Comparing these values of E and W with the curves presented in Figure 4.2, it may be seen that the error incurred by using the flat front model for modeling heat pipe injection lances is extremely low - on the order of 1 pipe radius length of error in estimating the inert gas shut-off zone.

5

The Transparent Heat Pipe

5.1 Introduction and Motivation

A low-temperature, laboratory-scale, transparent heat pipe injection lance was constructed and tested in order to investigate the validity of the assumptions invoked in the flat-front model. In particular, the following questions were to be answered :

1) How realistic is the assumption of an ideal flat-front temperature profile ?
2) Given a certain set of boundary conditions, can the inert gas / vapor front become "tilted" as suggested by Coscia [1] (p.26) ?
3) What is the effect, if any, of the use of different inert gases ?
4) What factors influence the onset of diffusion freeze-out ?

5.2 Apparatus

The thermosyphon tube was constructed from 1 mm gauge pyrex according to the geometric specifications illustrated in Figure 5.1.

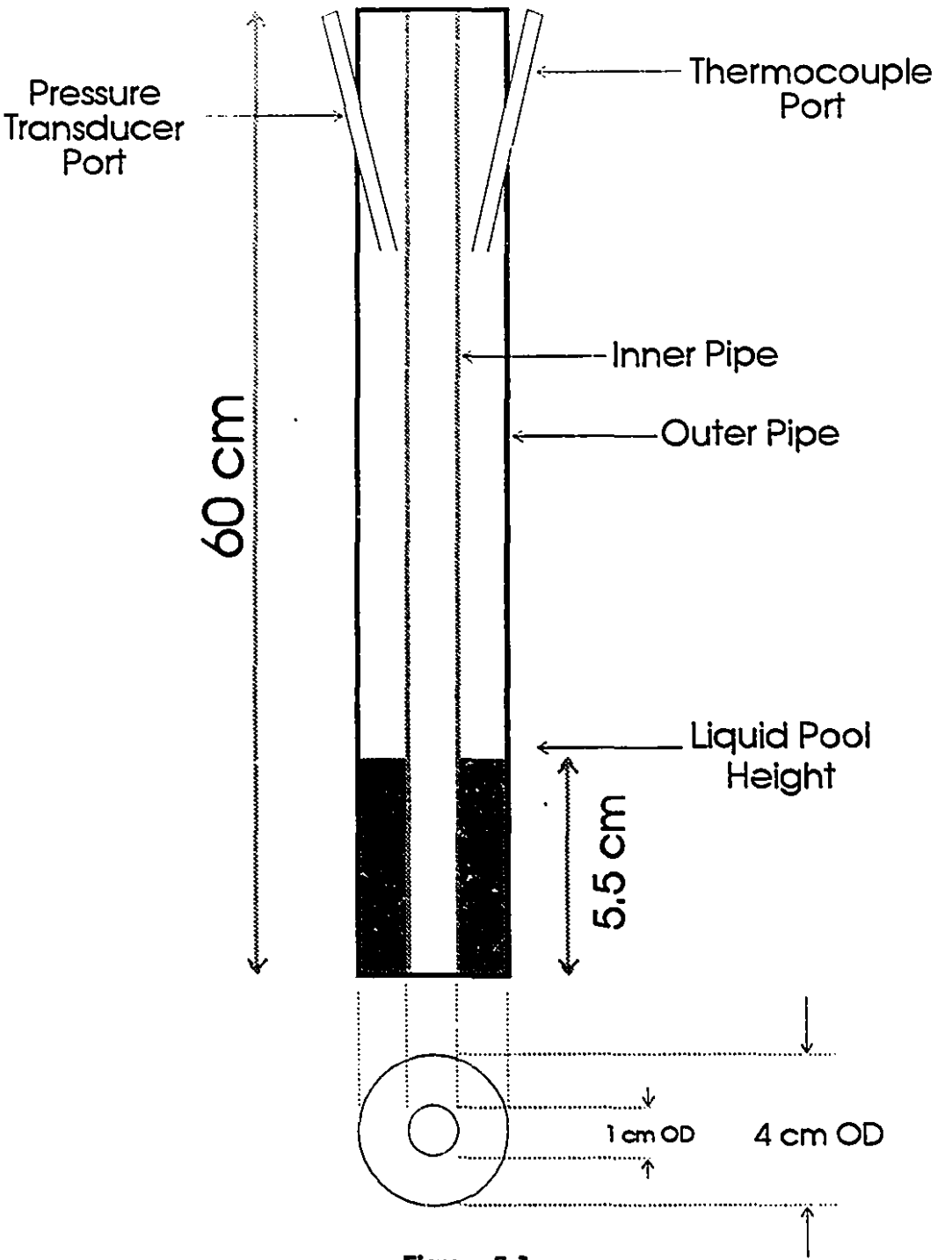

Figure 5.1
Pyrex Thermosyphon Tube

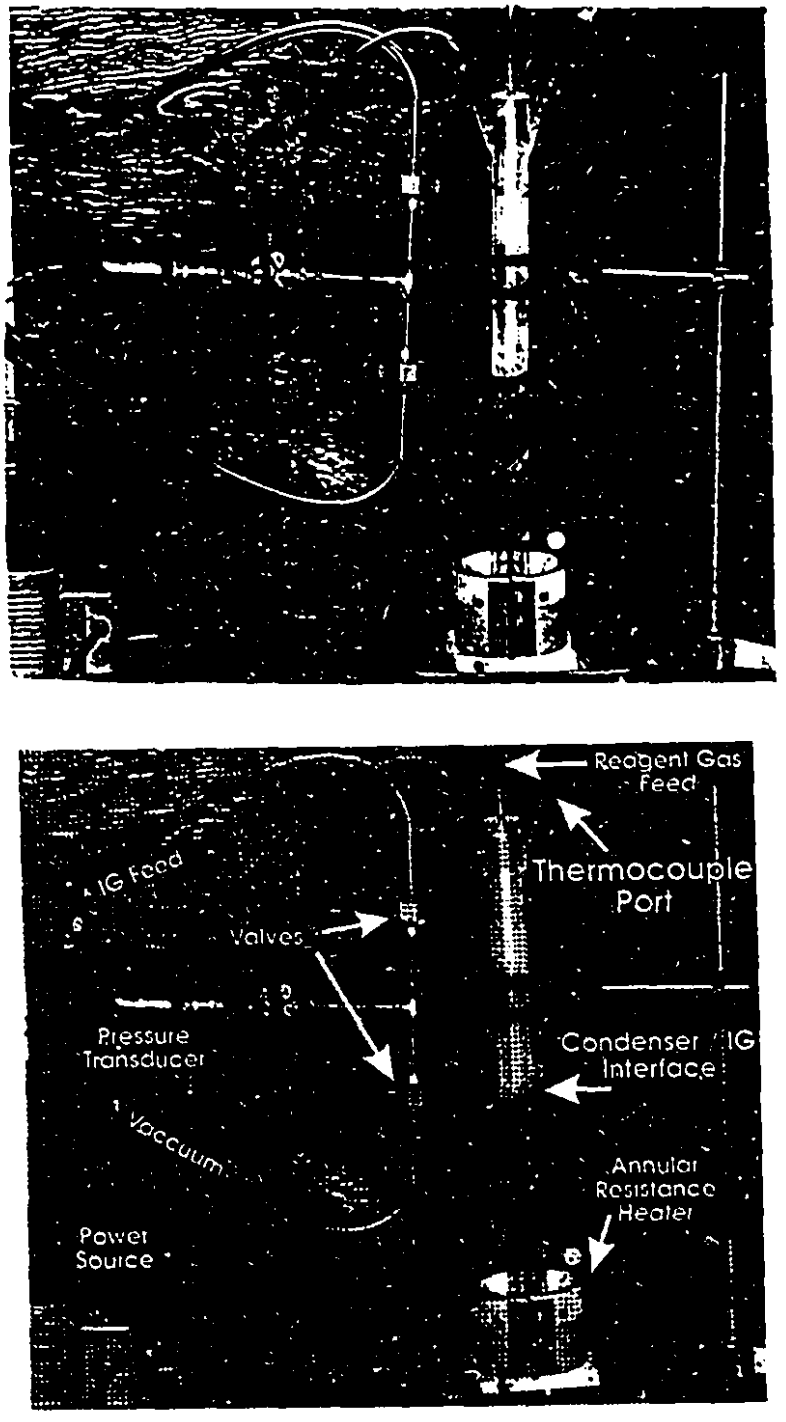

Figure 5.2
Pyrex Tube and Peripherals

Figure 5.2 illustrates the complete experimental setup used to test the pyrex thermosyphon injection lance. The reagent gas used was air, supplied under pressure from a standard wall outlet and fed into the central core of the pipe. The power source consisted of an AC-driven heating coil with variable voltage input indexed from 1 to 100.

The outer annulus of the pipe was accessible through the two small ports which, during pipe operation, served as access points for the pressure transducer and the thermocouple. The pressure monitoring port also served the vacuum line and the inert gas inventory line. These lines were sealed off during pipe operation. The sealed line connections were made using Swagelok ™ fittings, segments of ¼ inch OD stainless steel tubing, and ¼ inch ID plastic tubing fastened with steel tension bands. The tip of the thermocouple wire was inserted into the tube and fastened into place with a Swagelok ™ reducing union. Once in place, a special nylon fitting allowed the tip of the thermocouple to be moved axially without compromising the seal. Once sealed, the system remained airtight for all tested internal pressures between .01 and 5 atmospheres.

5.3 Working Substance Selection

Because of their commercial availability, surface wetting characteristics and desirable thermodynamic properties, water, Dowtherm A, acetone, methanol, ethanol, and refrigerants such as R11, R113, R22, R115 and R13B1[iv] are working substances commonly employed in low temperature heat pipe research. However, due to the low

freezing points of these substances, none of the above listed fluids allow the study of diffusion freeze-out at normal ambient conditions. Therefore, a fluid with a higher melting point than conventional low-temperature heat pipe working fluids was sought. According to this criterion, naphthalene ($C_{10}H_8$) was selected as the working fluid used for the experimental program conducted with the pyrex thermosyphon.

Naphthalene is a commercially available hydrocarbon known best as the distinctively malodorous constituent of the common mothball. To this author's knowledge, no experimental work utilizing naphthalene-loaded heat pipes has been published to date. Some properties of naphthalene are listed in Table 5.1.

NAPHTHALENE, $C_{10}H_8$	
Molecular Weight	128.1 grams.
Density (@ 20° C)	1.145 Kg/l.
Melting Point	80.2 °C.
Boiling Point at 1 atm.	217.9 °C.
Consistency of solid phase	Chalky, Opaque, White.
Consistency of liquid phase	Transparent.

Table 5.1
Properties of Naphthalene

Through the pyrex tube's charging ports, the lance was charged with sufficient quantities of naphthalene to bring the evaporator's liquid pool height to 5.5 cm prior to pipe startup.

Preliminary experiments indicated that the naphthalene, in liquid phase, readily wetted the pyrex tube and produced a stable condensate film. Naphthalene precipitate was found to be chalky and opaque, and thus readily distinguishable from the transparent liquid phase by a cursory visual examination. This property would prove to be extremely important in the experimental observation of diffusion freeze-out which followed.

5.4 Inert Gas Selection

During steady-state thermosyphon operation, the segregation of vapor and inert gas is produced by the convective force of the migrating vapor. While convection dominates the fluid flow regime close to the evaporator, the low vapor velocities in the vicinity of the vapor/inert gas interface area allows some diffusion to take place. In general, pressure-driven convective forces abet the creation of a sharp interface while diffusive forces have the opposite effect.

A third important force, however, can have a decisive effect on the integrity of the interface. This force is the gravitational *body* force which acts on both the vapor and gas. If the vapor has a higher density than the inert gas, then buoyancy forces will tend to abet the presence of a sharp, stable interface. On the other hand, if the inert gas has a greater density than the vapor, severe instabilities may arise at the interface. At points, pockets of inert gas may sink well below the interface area and cool the vapor in the immediate vicinity. This, in turn, may give rise to homogenous precipitation within the vapor flow and a localized depletion of the vapor, thereby causing a pressure

drop and an exacerbation of the instability. This can lead to the complete breakdown of the interface.[iv]

For this reason, three inert gases with different densities were tested. The tested gases are listed in Table 5.2. For naphthalene, $\rho_{v,atm}$ is 3.177 Kg / m^3.

Inert Gas	$\rho_{ig,atm}$	$\rho_{v,atm} / \rho_{ig,atm}$
Helium	0.166 Kg / m^3	19.14
Air	1.195 Kg / m^3	2.65
Sulfur Hexafluoride (SF_6)	6.071 Kg / m^3	0.52

Table 5.2
Inert Gases and their Densities

5.5 Temperature Profile

As discussed previously, the flat-front model invokes the assumption that the axial temperature and inert gas concentration profiles within the pipe may be expressed as step functions. This assumption was tested using the pyrex thermosyphon.

5.5.1 Experimental

The pyrex tube was loaded and tested with air, helium and SF_6. In the case of air, the pressure transducer port was left unsealed, allowing the system to operate at

ambient atmospheric pressure. In the case of helium and SF_6, it was necessary to seal the pressure port so that the inert gas composition would not become diluted by infiltrating air. The gas-loading, in these two cases, was done is such a fashion that the system operating pressure would be approximately atmospheric.

For the three tests, the variable supply voltage setting was set to 60 and no reagent gas flow was administered. Prior to temperature measurement, the system was allowed ample time to achieve steady state. The tip of the thermocouple probe was then positioned axially within the outer annulus so that the axial temperature profile could be observed.

5.5.2 Results

Radial temperature variations, for all three gases, were found to be negligible. In the case of He and air, no unsteady variations in temperature profile were observed. In the case of SF_6, however, transient local fluctuation were often severe. Data collected for the SF_6 loaded pipe, therefore, was time-averaged over a span of 2 minutes per data point. Figure 5.3 illustrates the temperature profiles observed.

Figure 5.3 illustrates that in the case of air and helium loading, segregation of the hot vapor from the cool inert gas is quite pronounced. In the case of SF_6, however, the countervailing buoyancy forces have severely disfigured the step profile.

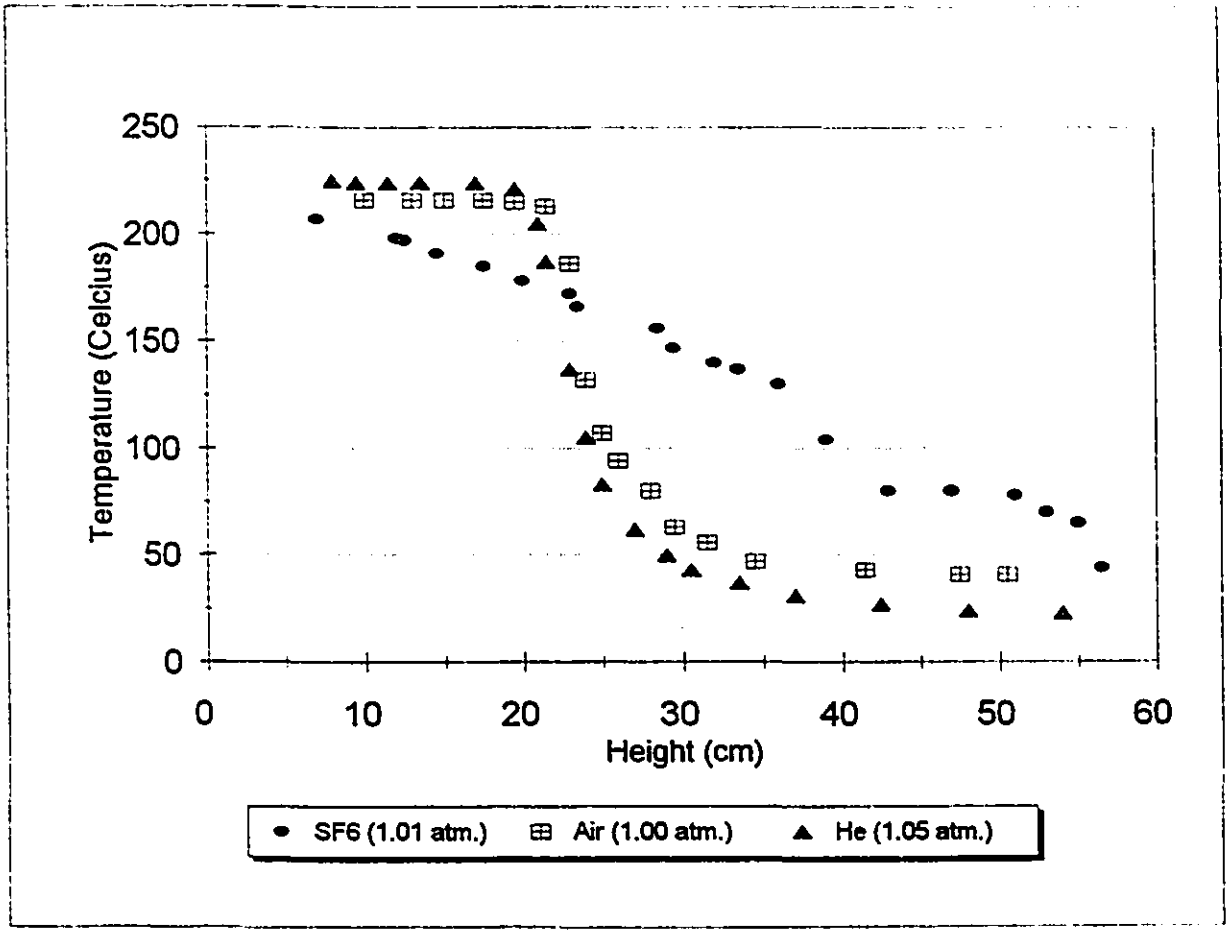

Figure 5.3
Temperature vs. Height for 3 Different Inert Gases

5.6 Flow Field Visualization

5.6.1 Pipe Loaded with Air and Helium

For the air and He-loaded pipes, condensation "rings" were observed demarcating the transition point from the vapor-rich region to the gas-rich region. These rings were observed on both the outer and inner pipes, and their position relative to each other allowed a determination of the shape of the front region. In the case of the rings observed on the outer pipe, they were typically situated 1-2 cm below the lowest diffusion freeze-out precipitate which had collected on the outer pipe. In the case of the rings which developed on the inner pipe, they were typically located less than 1 cm below the lowest diffusion freeze-out precipitate which had collected on the inner pipe. Figure 5.4 and Table 5.3 illustrate the slanted nature of the interface at various boundary conditions.

Experimental Run	Reagent Gas Air Flow (m/s, air at S.T.P.)	$Z_{\ell,i}$ (m)	Angle of Interface Inclination
a	0.0	.000	0°
b	30.5	.012	38.7°
c	63.0	.031	64.1°
d	111.0	.038	68.5°

Table 5.3
Interface Geometry at Different Flowrates for Air loaded pipe, 1 atm.

Figure 5.4 and Table 5.3 illustrate that even at very high reagent gas flowrates, and the correspondingly high heat flow extracted at the wall of the internal pipe, the disfiguration of the interface region is minimal. Vertical deflection of the front region is on the order of 1 pipe diameter. As such, the experiments with light inert gases ($\rho_{v,atm}/\rho_{lg,atm} > 1$) indicate that the assumption of a flat-front is valid *even in those cases where the disparity between ambient and inner pipe boundary conditions is considerable.*

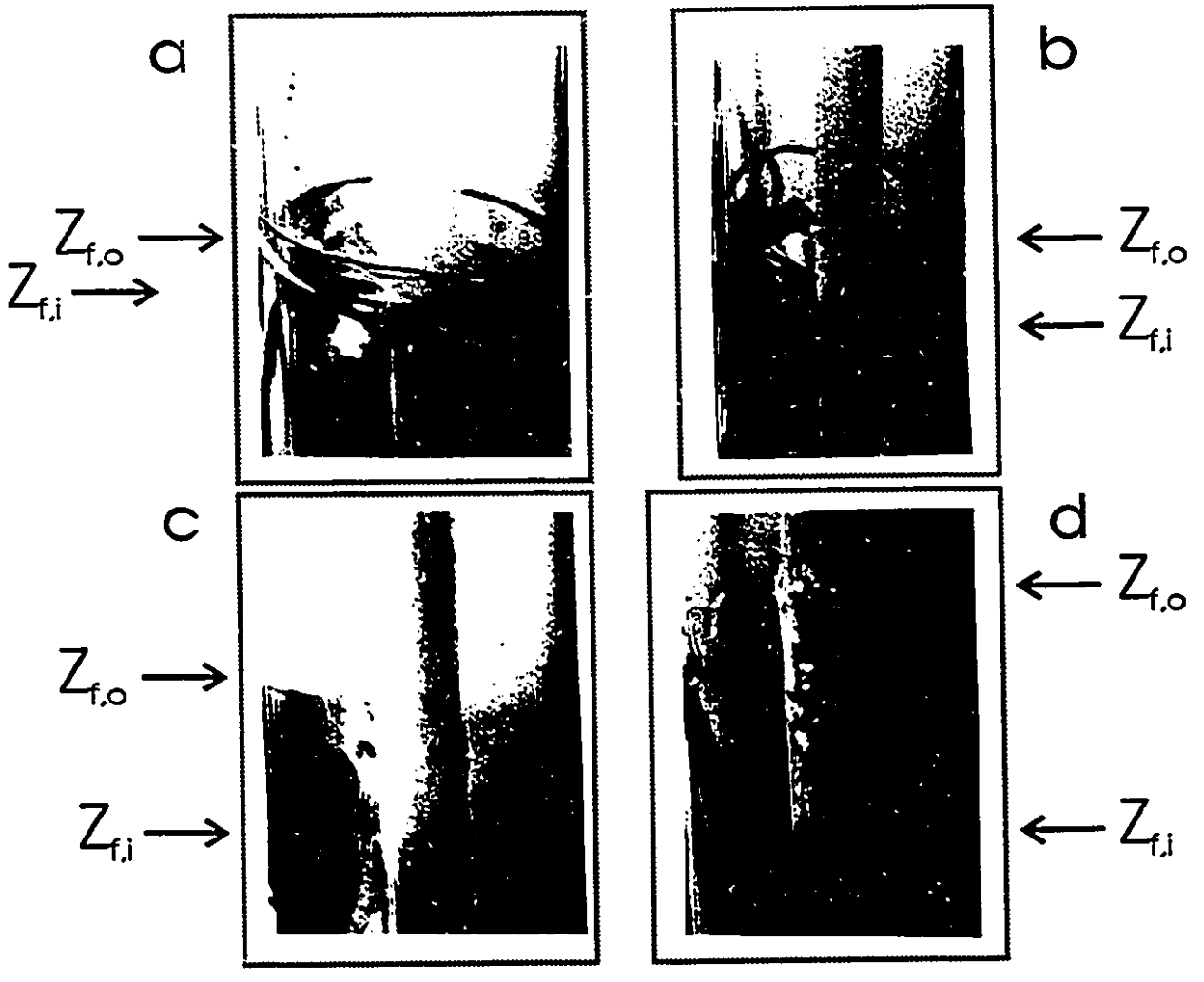

Figure 5.4
Interface Region for 4 Different Flow Conditions (Table 5.3)

• 5.6.2 Pipe Loaded with SF_6

Figures 5.5 and 5.6 illustrate the difference between the flowfield behavior in an air-loaded ($\rho_{v,atm}/\rho_{ig,atm} > 1$) and an SF_6-loaded pipe ($\rho_{v,atm}/\rho_{ig,atm} < 1$). In both cases, pipe pressure was 1.0 atm., voltage level was set to 55, and reagent gas velocity was 45.0 m/s. In the air-loaded pipe, as with the He-loaded pipe, buoyancy forces abet convective forces in the establishment of a stable, near-horizontal interface. However, no clear interface exists in the SF_6 loaded pipe. This absence, illustrated numerically in the near-uniform temperature decay presented in Figure 5.3, is illustrated graphically in Figures 5.5 and 5.6 below.

Since there is no discrete interface region in the SF_6-loaded pipe, the characteristic interface "rings" observed in the presence of a light inert gas are absent. While the interface regions in the presence of both air and He were highly stable, the same could not be said for the SF_6-loaded pipe. Large oscillations in the rate of vapor-phase condensation were observed, giving rise to pressure fluctuations and unsteady flows, including vortex flows. The absence of any discrete front allowed a copious recirculation flow of vapor and inert gas. This, in turn, produced a high solid-phase deposition rate towards the upper extremity of the pipe.

A B C

Figure 5.5
Air-Loaded Pipe (A) Exhibiting Steady Flow Behavior and
SF_6-Loaded Pipe (B and C) Exhibiting Unsteady Flow Behavior

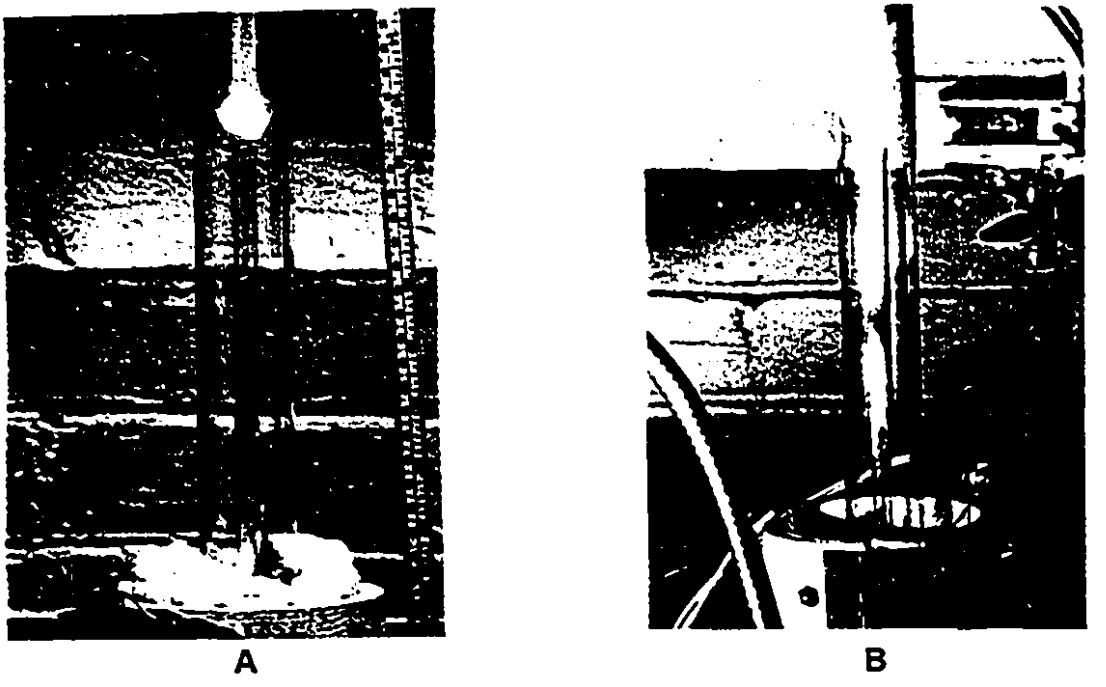

A B

Figure 5.6
Solid Phase Precipitation after 10 minutes of Operation
in Air-Loaded Pipe (A) and SF_6-Loaded Pipe (B)

5.7 Pyrex Heat Pipe Endurance Tests

Endurance tests were staged in order to determine the effect of inert gas selection on total elapsed time till the onset of complete diffusion freeze-out.

As Figures 5.7 and 5.8 illustrate, the effect of the $\rho_{v,atm}/\rho_{ig,atm}$ ratio is a critical factor with regard to the rate of solid phase precipitation within the pipe. In the case of air ($\rho_{v,atm}/\rho_{ig,atm} > 1$), the presence of the well-defined front interdicts the migration of vapor to the cold upper extremity of the pipe. The absence of such a well-defined front permits much faster liquid pool depletion in the case of SF_6. With both gases, the higher voltage level (Figure 5.8) rendered slower dry out times than with the lower voltage level (Figure 5.7). This was due to the fact that the unheated area available for solid phase precipitation is inversely proportional to the condenser height (which is itself a positive function of heat load).

Given these results, it is relevant to consider the Mark I lance of Botos discussed in Chapter 2. The Mark I lance employed sodium as a working substance ($\rho_{v,atm}$ = .243 kg/m^3) and nitrogen as the inert gas ($\rho_{ig,atm}$ = 1.16 kg/m^3). For this lance, the $\rho_{v,atm}/\rho_{ig,atm}$ ratio was 0.209, much lower than even the 0.52 ratio of the tested SF_6/naphthalene combination. In terms of slowing the onset of diffusion freeze-out in such high temperature applications, the use of helium ($\rho_{ig,atm}$ = .166 kg/m^3) instead of nitrogen presents obvious advantages.

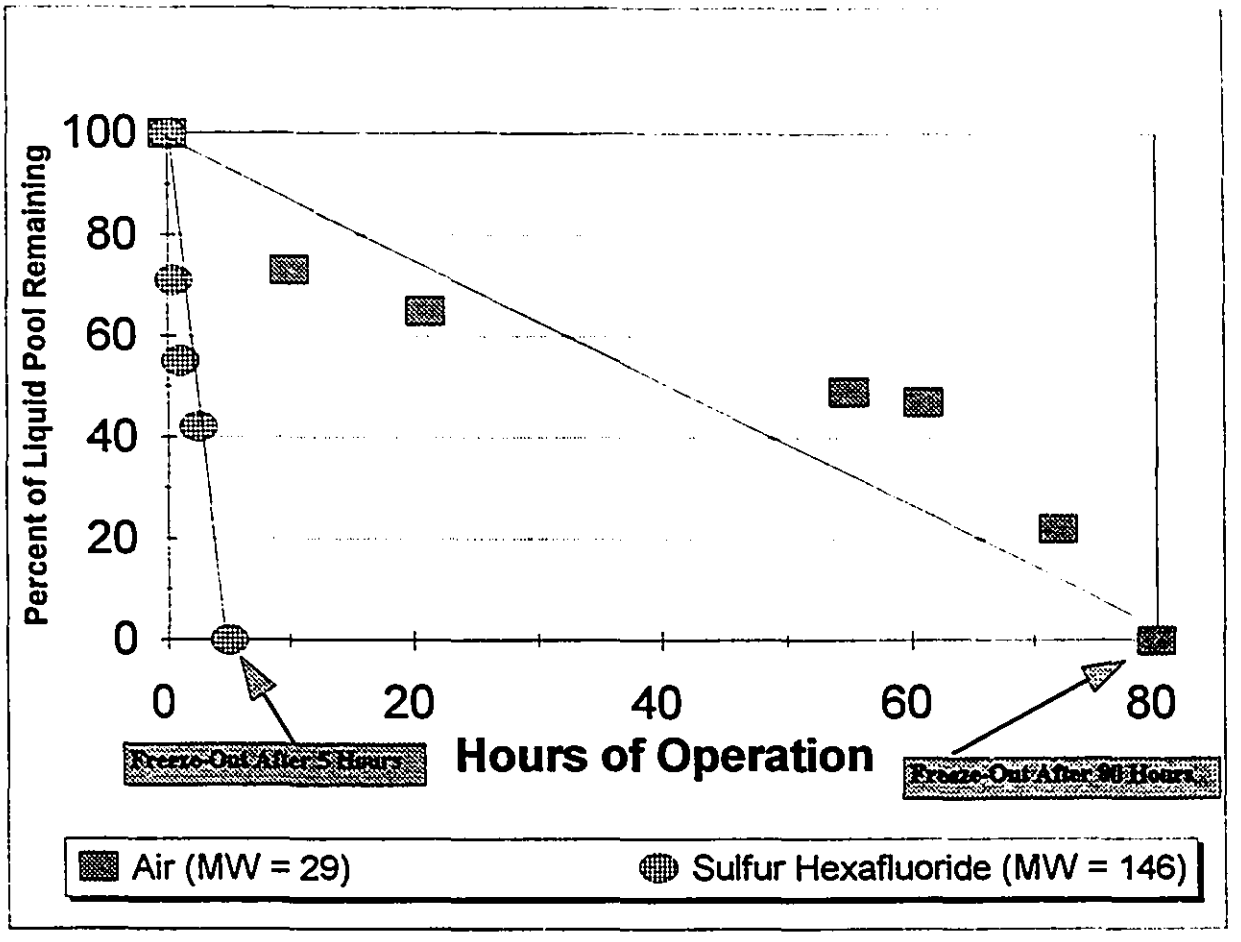

Figure 5.7
Percent of Liquid Pool Remaining vs. Time
for Voltage Level = 55

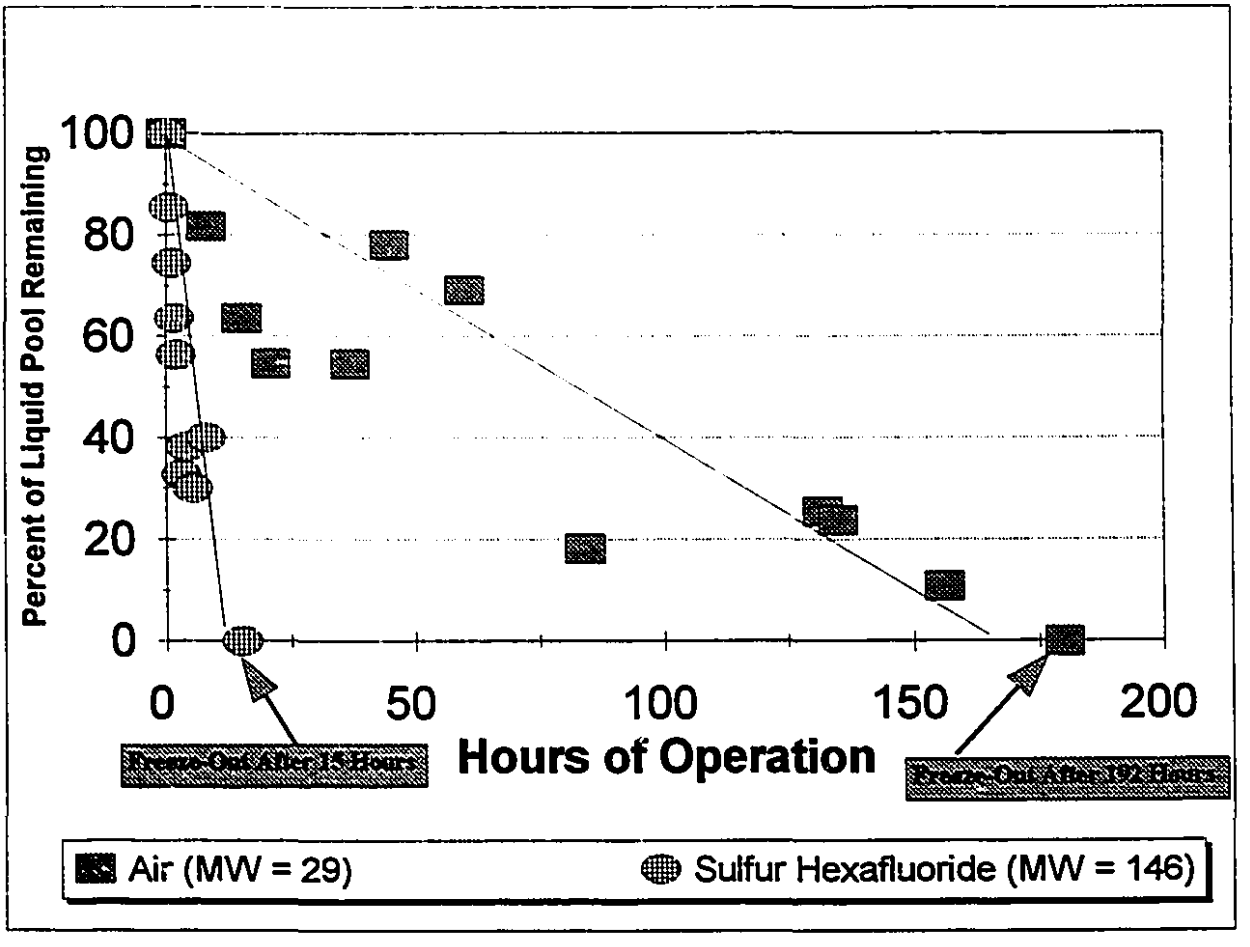

Figure 5.8
Percent of Liquid Pool Remaining vs. Time
for Voltage Level = 65

5.8 Pipe Wetting at Evaporator

As discussed, it is desirable for the working substance condensate to wet the pipe's hot internal surfaces. This is particularly important in the evaporator section of the heat pipe. In the non-wetting case, sections of the evaporator wall will not be protected by the condensate film and dry "hot spots" will emerge. These spots can, in the worst case, lead to pipe failure.

Hot spots emerge due to the conjugate effect of vapor/film shear stresses and high wall heat flux. As such, they are most likely to be found in the evaporator, above the top of the liquid pool. In the case where evaporator boundary conditions vary azimuthally, the hot spots are most likely to appear at the points where the heat flux is highest. The liquid is shunted to rivulets which circumnavigate the points of high heat flux. The formation of a hot spot resulting from high vapor/liquid shear stress and locally varying heat flux is schematized in Figure 5.9.

Figure 5.10 illustrates the appearance of hot spots in the pyrex thermosyphon at high heat load (voltage = 85).

This problem of hot spots can be eliminated if the condensate flow is protected from the shear force of the vapor in the presence of the applied heat load. This may be accomplished by using several wraps of fine metal mesh to line the inside of the pipe in the evaporator region.

A 5-fold wrapping of 100-mesh (150 μm) stainless steel mesh was used in the pyrex thermosyphon to successfully eliminate the onset of hot spots. This practice is illustrated in Figure 5.11.

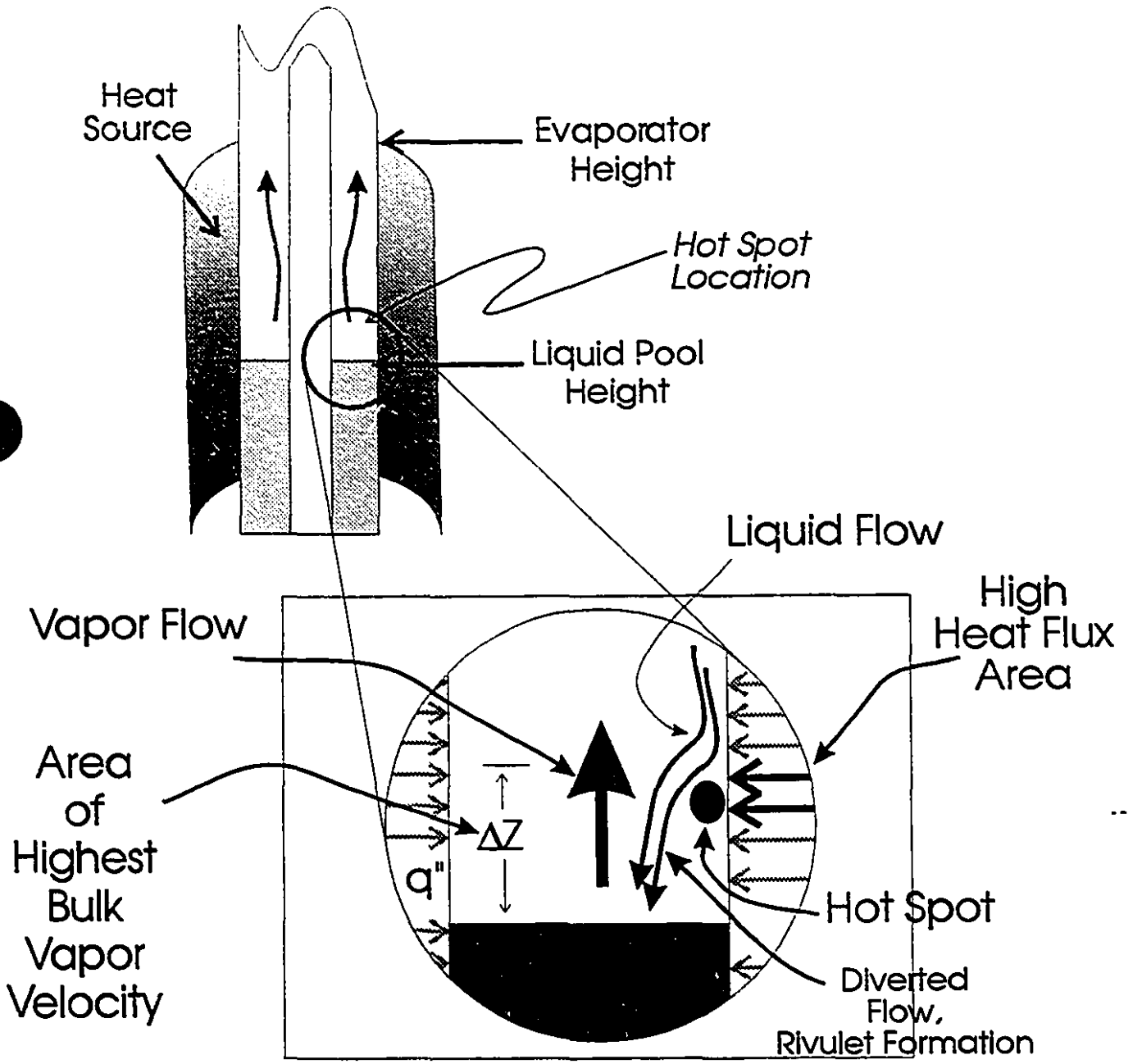

Figure 5.9
Likely Location of Hot Spots in a Heat Pipe

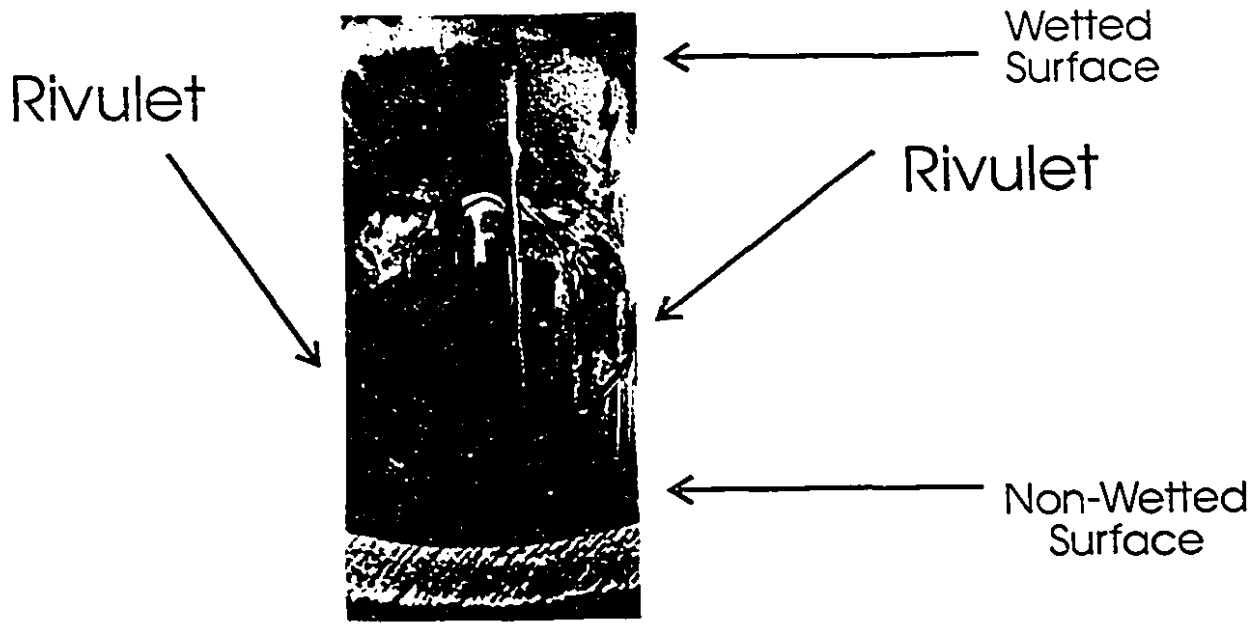

Figure 5.10
Hot Spots in Pyrex Thermosyphon (Voltage Level = 85)

Figure 5.11
Elimination of Hot Spots in Pyrex Thermosyphon
Using 150 μm Stainless Steel Mesh (Voltage Level = 85)

6

HEATPIPE 1.0

HEATPIPE 1.0 is a control volume, finite difference software simulation package created to model the steady state behavior of annular reflux thermosyphon injection lances. HEATPIPE 1.0 employs the flat-front model discussed earlier in this volume. It has been used successfully at the McGill Metals Processing Centre in the design and analysis of heat pipes for a wide variety of applications.[xxiv, xxix] HEATPIPE 1.0 has been written in FORTRAN for MS-DOS PCs. The input and output interfaces have been created using HS-PRO II™ subroutines and utilities

Users of HEATPIPE 1.0 employ a graphical user interface in order to input the data pertaining to the pipe, working substance and boundary conditions of interest. The 57 unknowns are calculated iteratively using the well-known Newton-Rapheson method[lvi]. Model results are presented graphically to the user following the successful completion of a simulation.

6.1 Model Construction

6.1.1 Nodes

Vertically, the pipe is sectioned into 5 discrete areas. The *Inert Gas Section* contains no nodes because it is assumed that negligible heat transfer takes place in this zone. As is the case with the *Condenser Section*, the length of the Inert Gas Section is not known prior to implementation of the model. In a gas-loaded thermosyphon, the position of the gas/vapor front (and, thus, the lengths of the Inert Gas and Condenser sections) is an unknown parameter. Vertically, the condenser section contains 3 nodal slices. These 3 nodal slices are spaced evenly through the condenser section which, as mentioned, is of unknown length prior to solving the system. Different boundary conditions may be applied to each of the condenser's 3 nodal slices.

The *Adiabatic Section* and the *Evaporator Section* are both of known length. The Adiabatic Section contains 1 nodal slice. The Evaporator Section contains 2 nodal slices. The relative size of the control volumes associated with the two nodal slices in the evaporator may be changed freely, as may the boundary conditions associated with each.

The tip area of the pipe receives special consideration since this is the point where the maximum temperature in many lance applications may be found. Boundary conditions at the tip are independent of the boundary conditions implemented at the two axial control volumes of the evaporator.

Figures 6.1 and 6.2 illustrate the allocation of nodes in the HEATPIPE 1.0 model.

6.1.2 Heat Pipe Types

HEATPIPE 1.0 may be used to model *Type I* and *Type II* thermosyphons. In a Type I thermosyphon, the inert gas inventory is a fixed parameter and system pressure is unknown. In a Type II thermosyphon, the system pressure is fixed by adjusting the inert gas inventory. In this case, the precise inventory of inert gas contained within the pipe is a variable which must be solved for. In either case, the total number of system variables remains unchanged.

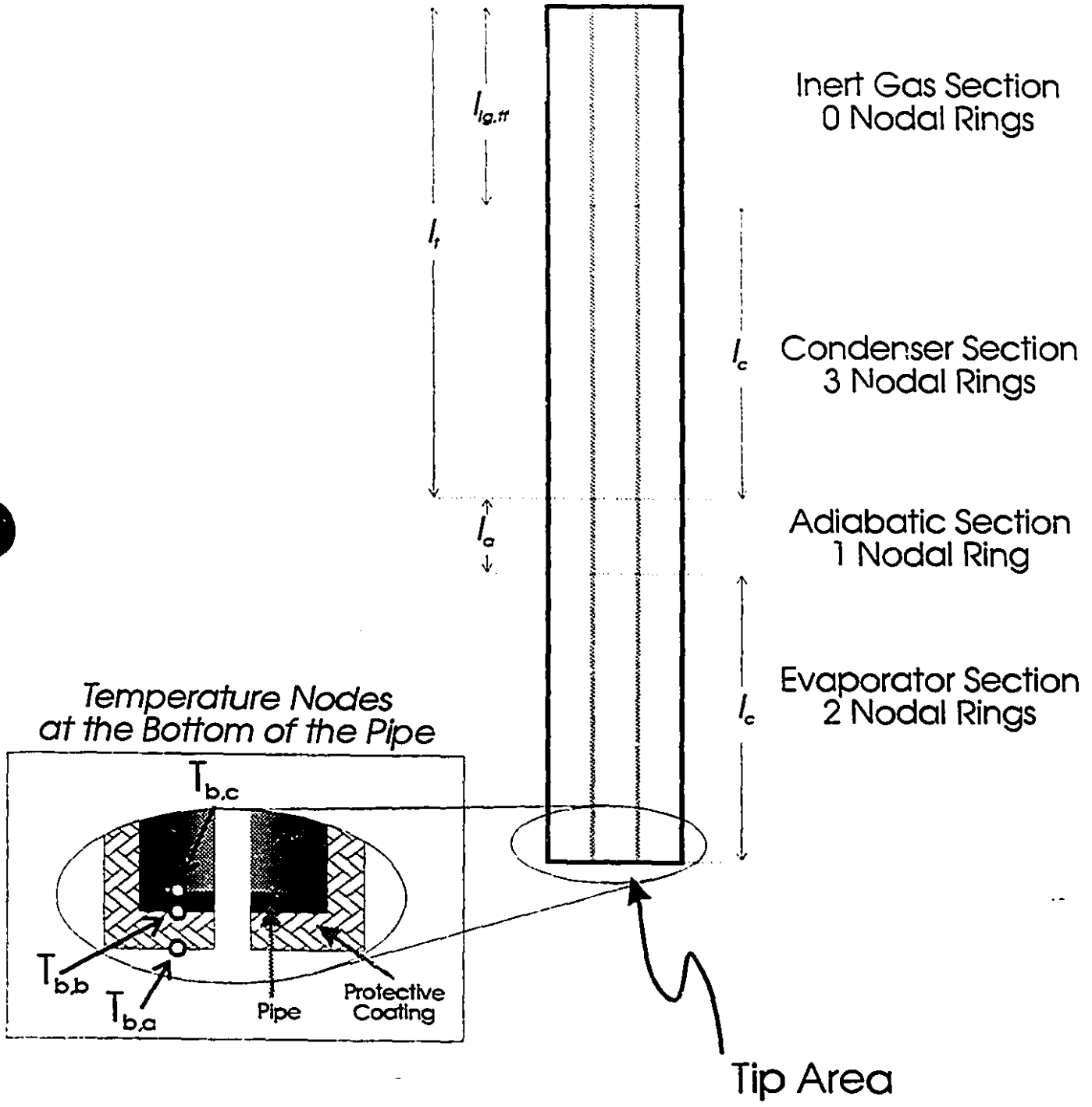

Figure 6.1
Vertical Sections and Allocation of Nodes in the HEATPIPE Model

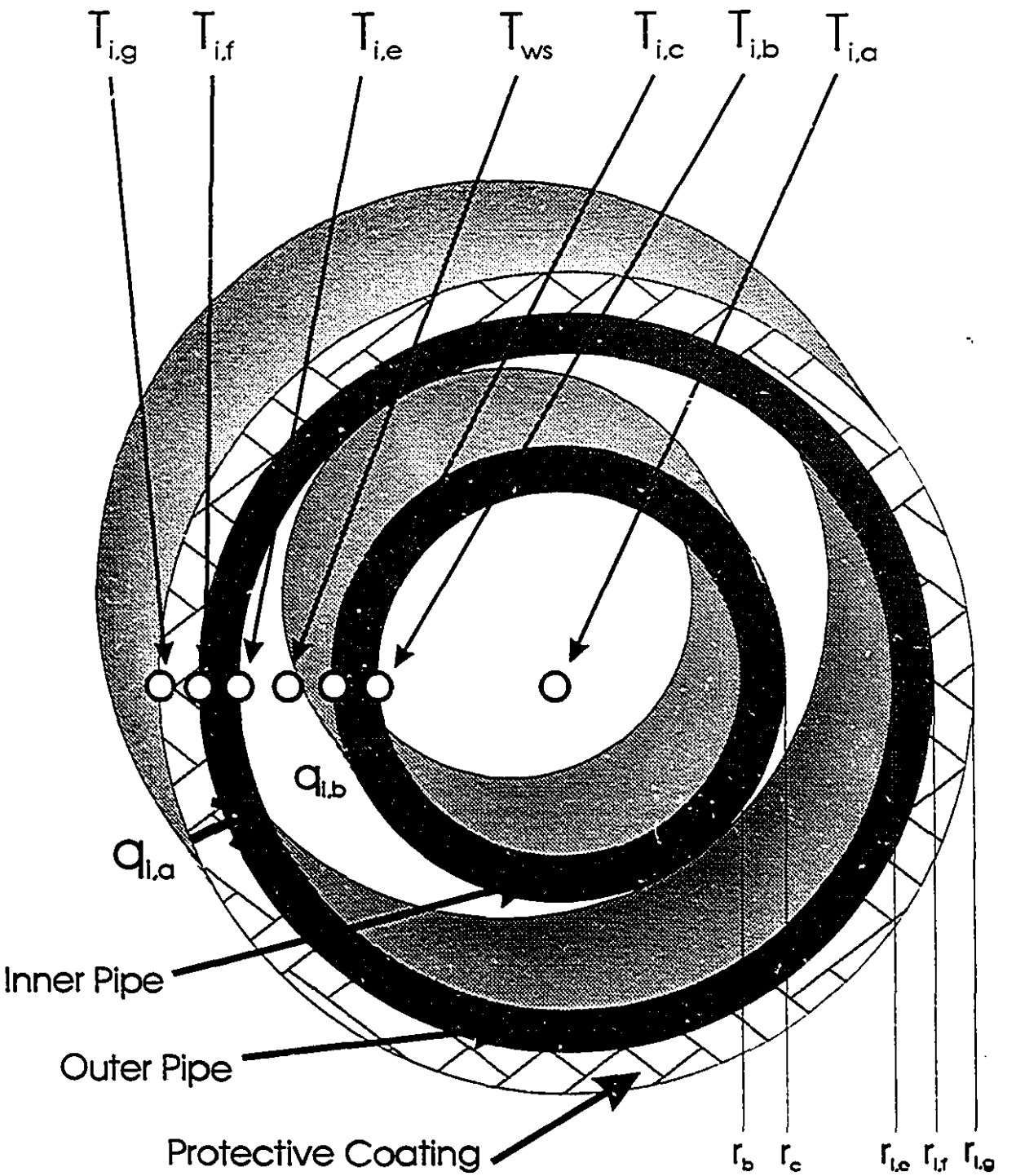

Figure 6.2
Cross-Section of a Nodal Ring in the HEATPIPE Model

• 6.1.3 Variables and Equations

HEATPIPE 1.0 uses user-input boundary conditions and material properties to solve a system of 57 equations and 57 unknowns. The unknowns are listed in Table 6.1

VARIABLES	DESCRIPTION	NUMBER
$q_{i,a}$, for i=1..6	Energy transfer from environment to working substance, ith node, W.	6
$q_{i,b}$ for i=1..6	Energy expelled from working substance to reagent gas, ith node, W.	6
q_{tip}	Energy absorbed by working substance through lance tip, W.	1
$T_{i,a}$ for i=1..6	Bulk temperature of reagent gas, ith node, K.	6
$T_{i,b}$ for i=1..6	Temperature of inner wall of inner pipe, ith node, K.	6
$T_{i,c}$ for i=1..6	Temperature of outer wall of inner pipe, ith node, K.	6
$T_{i,e}$ for i=1..6	Temperature of inner wall of outer pipe, ith node, K.	6
$T_{i,f}$ for i=1..6	Temperature of inner wall of protective coating, K.	6
$T_{i,g}$ for i=1..6	Temperature of outer wall of protective coating, ith node, K.	6
$T_{b,a}$, $T_{b,b}$ and $T_{b,c}$	Temperatures at bottom of the pipe, K.	3
l_c	Length of active condenser, m.	1
$l_{ig,ff}$	Length of blocked off region predicted by flat front model = $l_t - l_c$, m.	1
V_{ig}	Volume consumed by inert gas plug, m^3	1
T_{ws}	Temperature of working substance, K.	1
P (Type I pipe) or n_g (Type II pipe)	System pressure or Moles of inert gas contained in the pipe.	1
	Total	57

Table 6.1
Variables Employed in HEATPIPE Model

EQUATION	DESCRIPTION		NUMBER
q from environment, node i	$q_{i,a} = 2 \cdot \pi \cdot r_{i,a} \cdot l_i \cdot h_{i,env}(T_{amb,i} - T_{i,g}) + \beta \varepsilon F \cdot (T_{amb,i}^4 - T_{i,g}^4)$	Eq. 6.1	6
q through outer coating, node i	$q_{i,a} = 2 \cdot \pi \cdot l_i \cdot k_c \cdot \ln\left[r_{i,g} / r_{i,f}\right] \cdot (T_{i,g} - T_{i,f})$	Eq. 6.2	6
q through outer pipe shell, node i	$q_{i,a} = 2 \cdot \pi \cdot l_i \cdot k_s \cdot \ln\left[r_{i,f} / r_{i,e}\right] \cdot (T_{i,f} - T_{i,e})$	Eq. 6.3	6
q from outer pipe shell to working substance, node i	$q_{i,a} = 2 \cdot \pi \cdot r_{i,a} \cdot l_i \cdot h_{i,ws}(T_{i,f} - T_{ws})$	Eq. 6.4	6
q from working substance to inner pipe shell, node i	$q_{i,b} = 2 \cdot \pi \cdot r_c \cdot l_i \cdot h_{i,ws}(T_{ws} - T_{i,c})$	Eq. 6.5	6
q through inner pipe shell, node i	$q_{i,b} = 2 \cdot \pi \cdot l_i \cdot k_s \cdot \ln\left[r_c / r_b\right] \cdot (T_{i,c} - T_{i,b})$	Eq. 6.6	6
q into reagent gas, node i	$q_{i,b} = 2 \cdot \pi \cdot r_b \cdot l_i \cdot h_{gas}(T_{i,b} - T_{i,a})$	Eq. 6.7	6
q from environment, lance tip	$q_{tip} = h_{bottom} \cdot A_{bottom} \cdot (T_{env,tip} - T_{b,a}) + \beta \varepsilon F \cdot (T_{env,tip}^4 - T_{b,a}^4)$	Eq. 6.8	1
q through outer coating, lance tip	$q_{tip} = \dfrac{k_c \cdot A_{bottom} \cdot (T_{b,a} - T_{b,b})}{t_c}$	Eq. 6.9	1
q through outer pipe, lance tip	$q_{tip} = \dfrac{k_s \cdot A_{bottom} \cdot (T_{b,b} - T_{b,c})}{t_s}$	Eq. 6.10	1
q from outer pipe shell to working substance, lance tip	$q_{tip} = h_{tip,ws} \cdot A_{bottom} \cdot (T_{b,c} - T_{ws})$	Eq. 6.11	1
Reagent gas heat accum.	$q_{i,b} = \rho_i \cdot v_g \cdot A_g \cdot C_{p,gas} \cdot (T_{i,a} - T_{i-1,a}) - v_g \cdot A_g \cdot \dfrac{dP_{ws}}{dz}$	Eq. 6.12	6
Working Substance q Balance	$q_{tip} + \sum_{i=1}^{5}(q_{i,a} - q_{i,b}) = 0$	Eq. 6.13	1
Clausius-Clapeyron	$\ln\left(P_{ws} / 1013 \cdot 10^3\right) = \dfrac{a}{T_{ws}} + b$	Eq 6.14	1
Length Conservation	$l_{ig,ff} + l_c = l_t$	Eq. 6.15	1
IG Length / Volume Ratio	$V_{ig} = l_{ig,ff} \cdot (r_i^2 - r_c^2)$	Eq. 6.16	1
Ideal Gas Law	$P_{sys} \cdot V_{ig} = n_{ig} \cdot R \cdot T_{ig}$	Eq. 6.17	1
	Total		57

Table 6.2
Equations Employed in HEATPIPE Model

Table 6.2 lists the equations used to solve for the variables listed in Table 6.1. Equations 6.2, 6.3 and 6.6 represent the forms for steady 1-D radial conduction heat transfer for a circular cross-section. Equations 6.1 and 6.8 represent the forms for steady 1-D radiative and convective heat transfer to an exposed surface. Equations 6.4, 6.5, 6.7 and 6.11 represent the heat flow from a surface to a fluid by a purely convective mechanism. Equations 6.9 and 6.10 represent the conduction equation for a 1-D Cartesian system. Equation 6.12 represents the energy balance on the reagent gas with two terms: one representing the temperature increase in the gas, the other representing the loss of energy due to depressurization of the gas stream. Equation 6.13 represents the global energy balance on the working fluid. Equation 6.14 represents the relation between pressure and temperature which exists for a given working fluid. Equations 6.15 and 6.16 represent geometric identities. Equation 6.17 is the equation of state for the ideal gas.

6.2 Input

HEATPIPE 1.0 solves the steady-state representation of a thermosyphon injection lance using user-input parameters. The pipe geometry, heat transfer coefficients, radiative coefficients, reagent gas properties and working substance characteristics may all be stipulated by the user.

Figures on the following pages illustrate the interface employed by the user to input the various simulation parameters. Figures 6.3, 6.4, 6.5 and 6.6 illustrate, respectively, the *Main Menu screen*, the *Working Substance* screen, the *Boundary*

Condition screen and the *Pipe Configuration* screen for the simulation of a Type I, laboratory scale, oxygen top blowing injection lance for BOF steelmaking.

For each individual field in the various input screens, a special message bar at the bottom of the screen informs the user of the units of input and the maximum and minimum values which may be applicable. The F10 and ESC keys (or the corresponding icons) are used to either confirm or abort data input.

The input routines also contain basic error-checking features. For instance, entering an inner pipe, outer radius less than the inner pipe, inner radius is not permitted.

For the thermodynamic properties of the working substance (Figure 6.4) the user has the option of describing the equilibrium temperature-pressure relationship of the working substance vapor by means of entering either a non-atmospheric P-T point or the latent heat of evaporation of the substance. For the working substance screen, entry of the surface tension at the vapor-liquid interface is *not* a required input. This quantity is only required should the user wish to compute capacity-limiting heat flows.

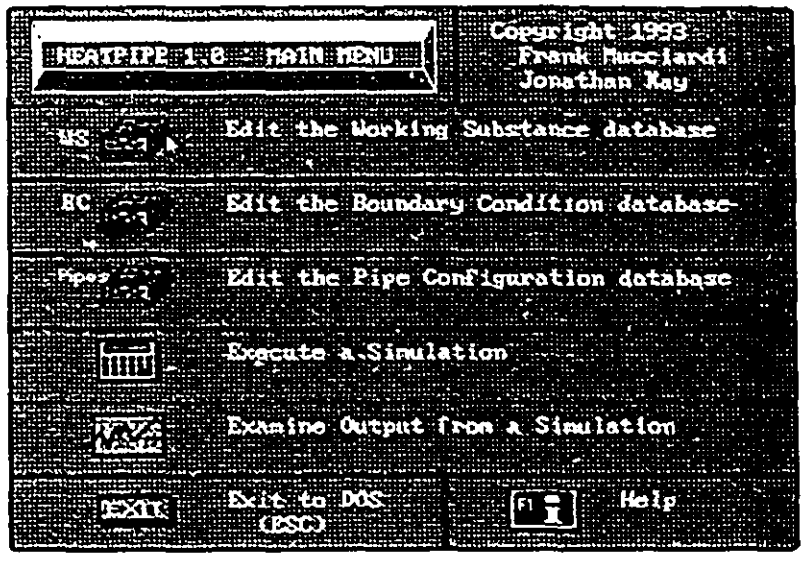

Figure 6.3
Main Menu Screen for HEATPIPE 1.0

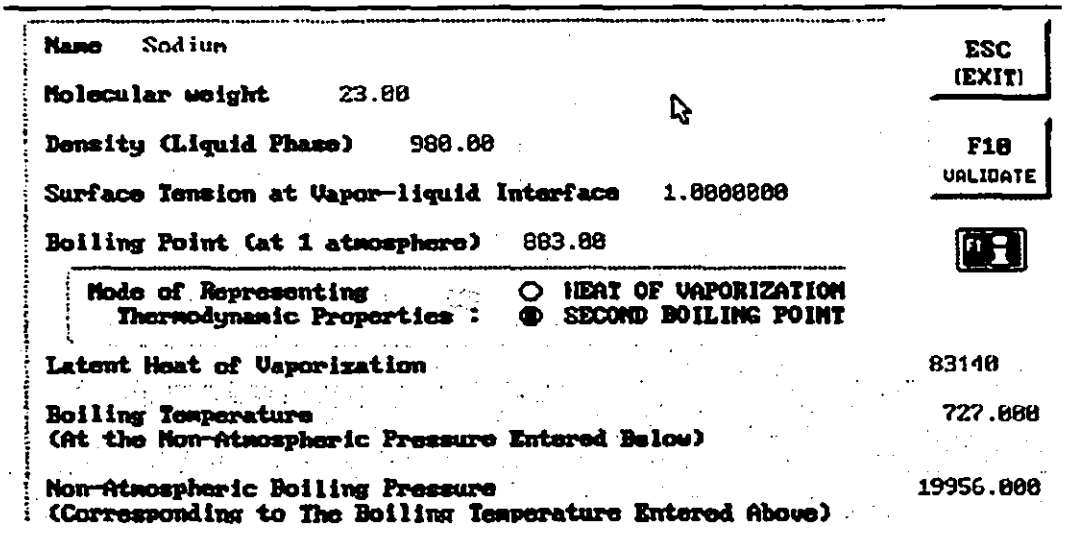

Figure 6.4
Working Substance Screen for HEATPIPE 1.0

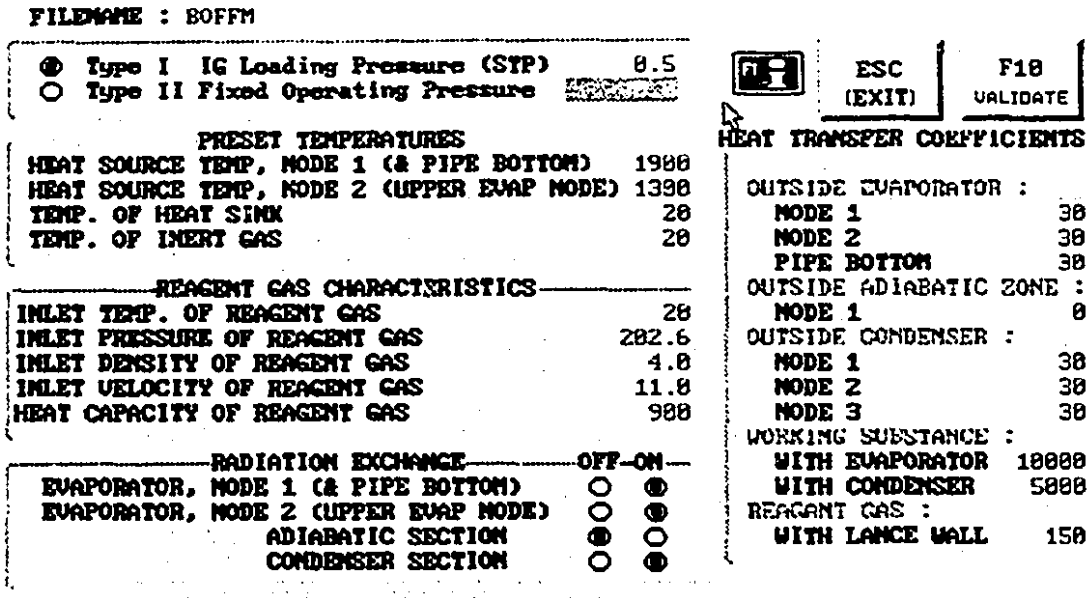

Figure 6.5

Boundary Condition Screen for HEATPIPE 1.0

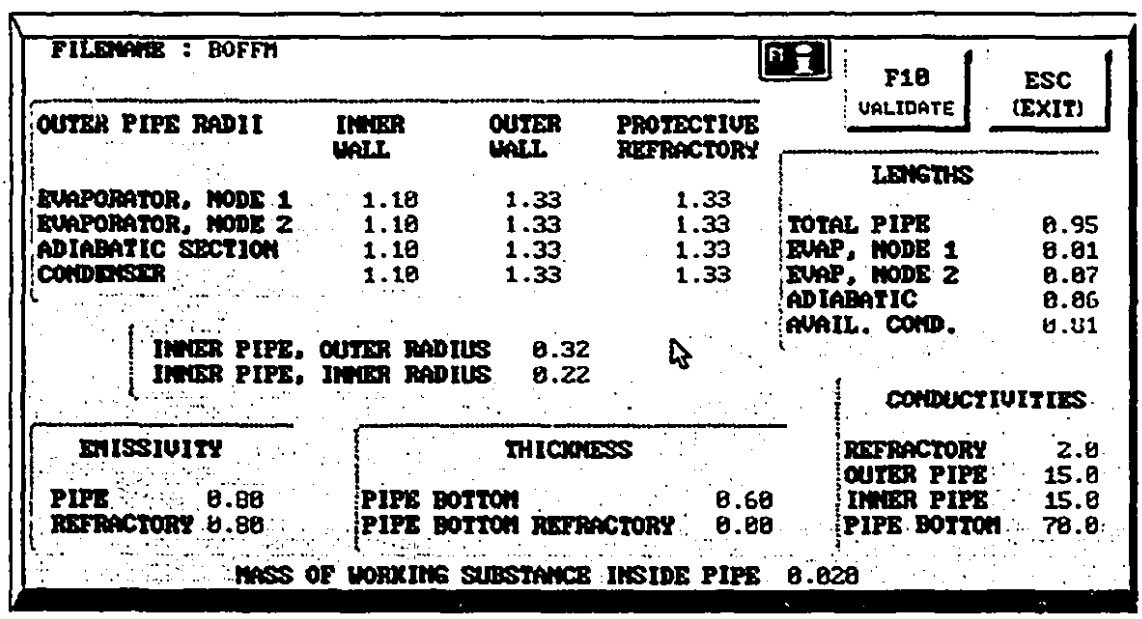

Figure 6.6

Pipe Configuration Screen for HEATPIPE 1.0

6.3 Computation

The information input by the user using the Working Substance, Pipe Configuration and Boundary Condition screens is combined to produce a simulation input file. Figure 6.7 illustrates the *Simulation Execution* menu, which allows the user to freely mix Boundary Condition, Working Substance and Pipe Configuration files. Thus, a user may retain a database of independent substances, pipes and environments which may be matched freely for any given simulation. The user is also free to select the mathematical threshold for the termination of the simulation and the maximum allowable iterations for an uninterrupted simulation run.

Figures 6.8, 6.9 and 6.10 illustrate the manner in which the user is updated during the iterative computation. In the case where a simulation remains incomplete, the user is asked whether he or she wishes to continue computation and, if so, for how many additional iterations. Extensive testing of the HEATPIPE 1.0 model has shown that the model will *always* converge for Type I pipes. Convergence for Type II pipes, however, is not guaranteed since the fixed system pressure does not allow for temperature variation in the working substance. For high heat loads in Type II pipes, even a situation in which $l_c=l_t$ may not allow sufficient evacuation of heat from the working substance. Under these circumstances, the model will not converge for Type II pipes. This non-convergence accurately reflects the non-viability of such a steady-state scenario under real physical conditions.

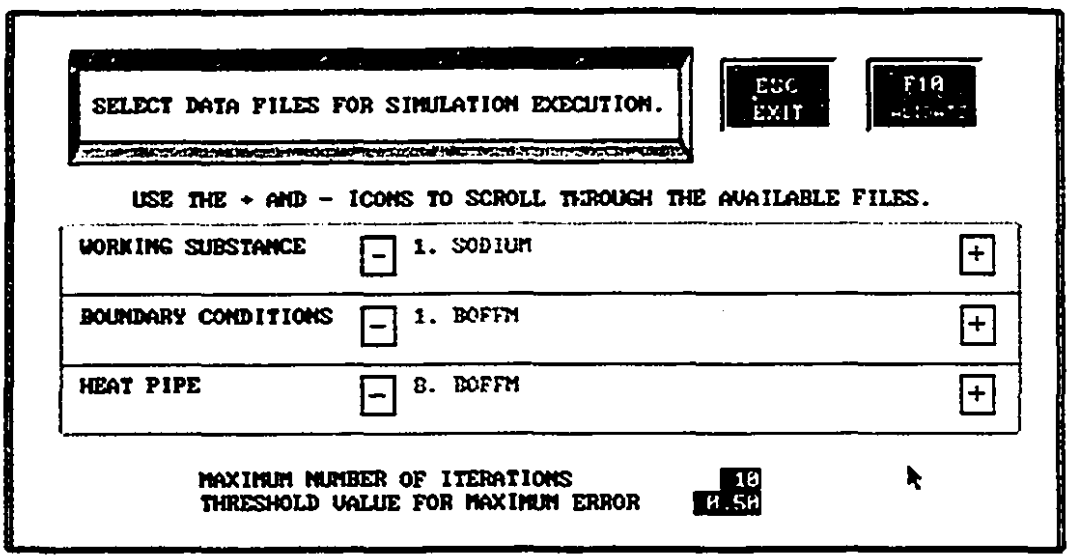

Figure 6.7
Simulation Execution Menu Screen for HEATPIPE 1.0

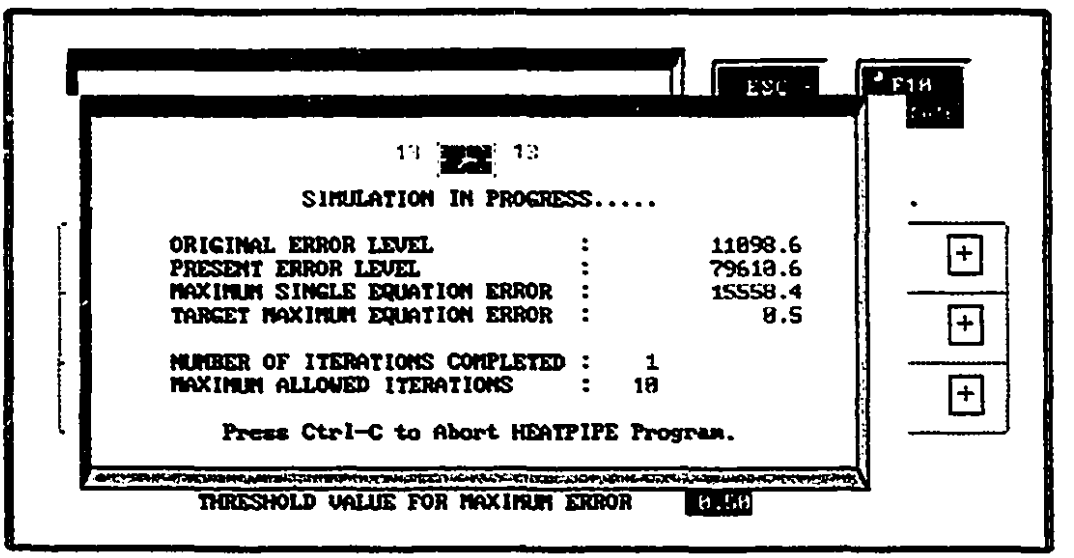

Figure 6.8
User Update Screen for HEATPIPE 1.0

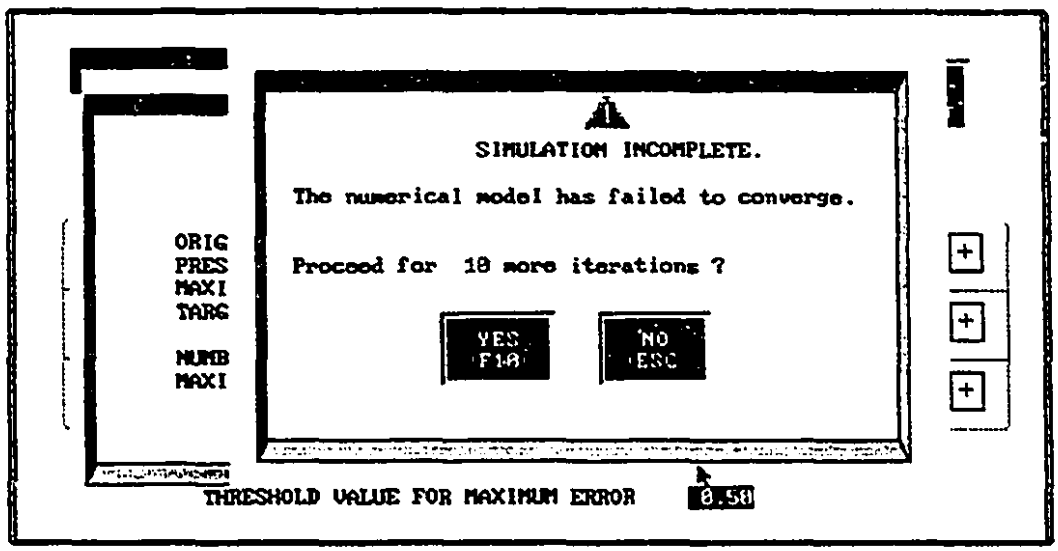

Figure 6.9
Additional Computation Prompt Screen for HEATPIPE 1.0

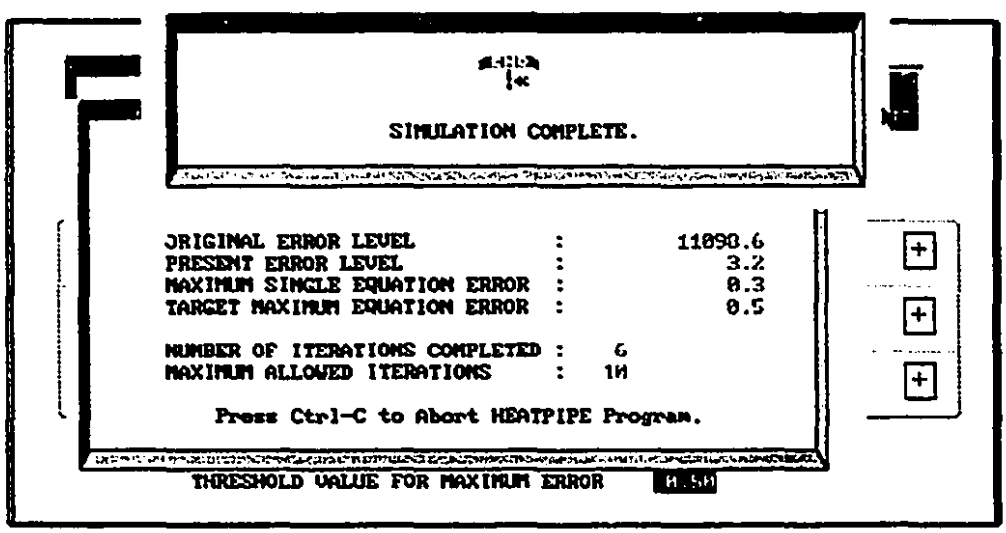

Figure 6.10
Successful Termination of Simulation Screen for HEATPIPE 1.0

6.4 Output

Following the successful termination of a simulation, the user may examine the values of the calculated variables. Figure 6.11 illustrates the *Output Menu* which the user employs to invoke the various output options. Figures 6.12 through 6.15 illustrate the various output screens for the input conditions illustrated in Figures 6.4 through 6.6. Figure 6.12 illustrates the output of the pipe's *Temperature Profile*. Figures 6.13 and 6.14 show the computed *Heat Flows* (Watts) and *Heat Fluxes* (Watts/m^2). Figure 6.15 illustrates the output of the main *System Parameters*. The system parameters screen may be output either to scale or "stretched" radially, as in the case of the temperature and heat flow/flux screens. The system parameters screen contains several quantities of interest, including, among other results, the maximum vapor velocity within the pipe, the percentage of heat recycled to the reagent gas, the percent of available condenser used and the total power extracted from the heat source.

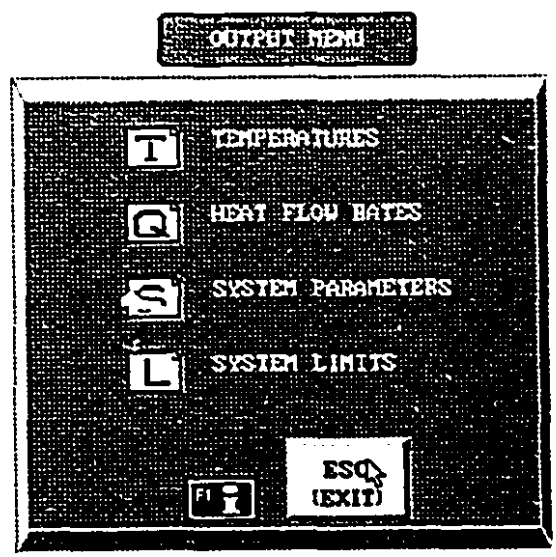

Figure 6.11
***Output Menu* Screen for HEATPIPE 1.0**

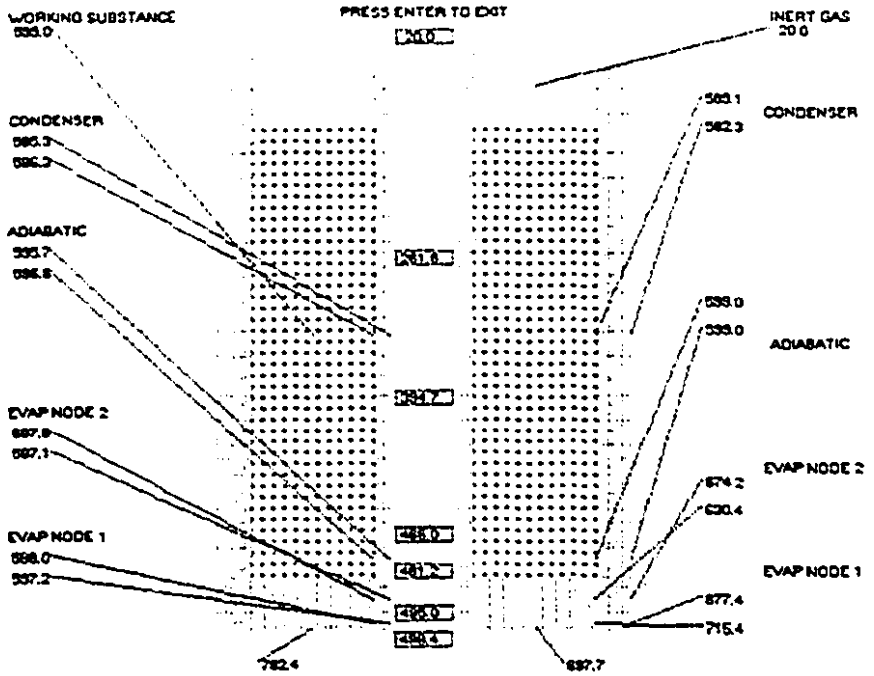

Figure 6.12
***Temperature Profile* Screen for HEATPIPE 1.0**

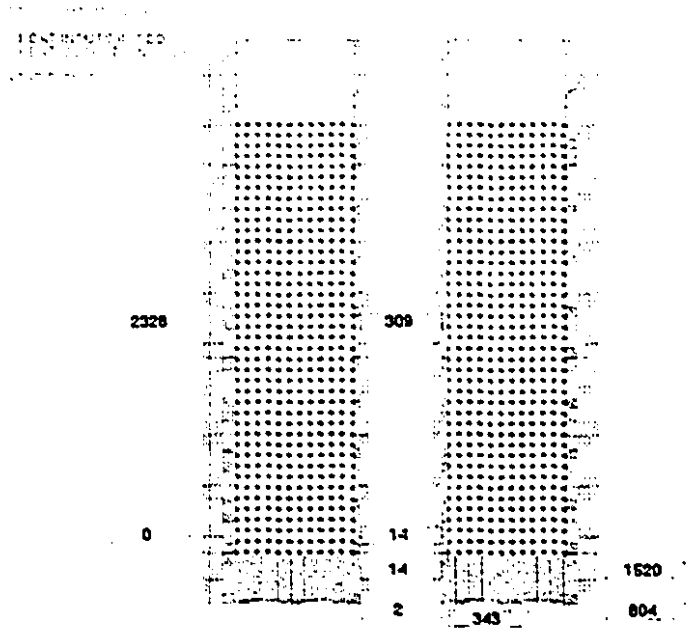

Figure 6.13
***Heat Flow* Screen for HEATPIPE 1.0**

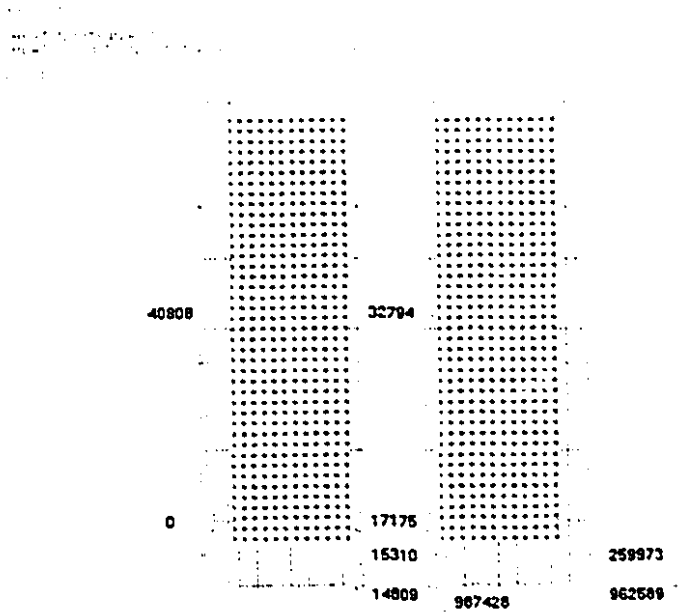

Figure 6.14
Heat Flux Screen for HEATPIPE 1.0

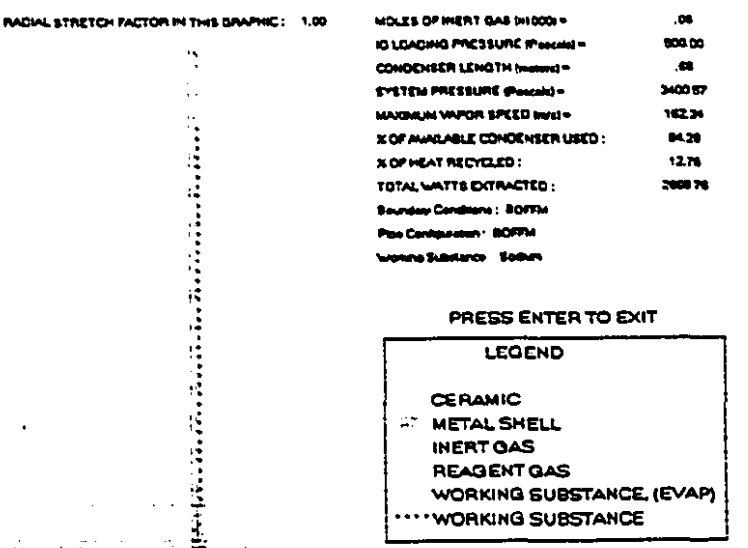

Figure 6.15
System Parameter Screen for HEATPIPE 1.0

6.5 Evaluation of Model Results

HEATPIPE 1.0 has been used successfully in the simulation of a novel heat pipe probe for the thermal analysis of aluminum casting alloys[xxv] and other applications[lvii,lviii]. HEATPIPE 1.0 has been particularly useful, however, in the design and analysis of laboratory-scale heat pipe BOF steelmaking lances. The data presented in Figures 6.4 through 6.15 represents actual input parameters and model results for the simulations run by Mucciardi et al. in parallel with the first heat pipe BOF experiments[xxx] in 1993. Table 6.3 illustrates the agreement between the predicted model results and the experimental data.

	Experimental Data (Mucciardi, Jin & Kay, 1994)	HEATPIPE 1.0	% Error
Reagent Gas Preheat (°C)	430.0	478.4	11.2
Evaporator Wall Temperature	870.0 °C 1143.0 K	877.0 °C 1150 K	0.6
Condenser Wall Temperature	559.0 °C 832.0 K	582.0 °C 855 K	2.8
% of Available Condenser Used	87.0	84.3	3.1
System Pressure (Pa)	3650	3400	6.8

Table 6.3
Results from Experimental Data and Computed Simulation

7

Conclusion

During my term of study at McGill, substantial and meaningful progress has been made toward implementing heat pipe technology in the metallurgical industry. Work conducted by myself and my colleagues at McGill have dramatically illustrated the advantages of heat pipes over conventional cooling systems. The computational utility which I have produced and the experiments which I have conducted are part of this larger research effort.

With regard to the experiments, there are 3 important conclusions which may be drawn:

1. The choice of inert gas is an extremely important parameter in gas-loaded thermosyphon operation. In order to produce a stable interface with minimal penetration of migrating vapor, the lightest possible inert gas should be selected. Helium, a gas which is non-reactive, extremely light and commercially available is a suggested choice for all applications.
2. For cases in which the density of the inert gas is less than the density of the working substance vapor, the deflection of the gas/vapor interface is minimal and the flat-

front model may be employed. This was found even when very large discrepancies existed between the boundary conditions presented at the external environment and those presented by the reagent gas flow.

3. A metal mesh liner should be used in the evaporator in order to avoid the onset of dry "hot spots" on the inner wall of the outer pipe.

Hopefully, this research will soon be conducted on a larger scale and the pace of integration of heat pipe technology into the metallurgical industry will accelerate.

References

[i] Botos, P., "The Heat Pipe Injection Lance", M. Eng. Thesis, McGill University, 1992.

[ii] Silverstein, C., Design and Technology of Heat Pipes for Cooling and Heat Exchange, 1992, Hemisphere Publishing Corp., Washington

[iii] Dunn, P.D., and Reay, D.A., 1982, Heat Pipes, 3rd ed., Pergammon Press, Oxford, pp 201-234.

[iv] G.P. Peterson, B.K. Bage, Entrainment Limitations in Thermosyphons and Heat Pipes, Journal of Energy Resources Technology, September 1991, Vol. 113.

[v] Roberts, C.C., A Review of Heat Pipe Delivery Concepts. Advances in Heat Pipe Technology. Proc. IV Int. Heat Pipe Conference, Pergamon Press, Oxford, 1981.

[vi] Wyatt, T., A controllable heat pipe experiment for the SE-4 satellite. JHU Tech. Memo. APL-SDO-1134, John Hopkins University, Applied Physics Lab., AD 695433, March 1965.

[vii] Katzoff, S., 1967, "Heat Pipes and Vapor Chambers for Thermal Control of Spacecraft," Thermophysics of Spacecraft and Planetary Bodies, ed. G.B. Heller, Academic Press, New York, pp. 761-818.

[viii] Marcus, B.D., 1971, "Theory and Design of Variable Conductance Heat Pipes, Research Report No. 2," TRW Report No. 13111-6027-RO-00.

[ix] Gaugler, R.S. Heat Transfer Device. US Patent 2350348, Published 6 June, 1944.

[x] Perkins, L.P. and Buck, W.E. Improvements in Devices for the Diffusion or Transference of Heat. UK Patent No. 22272, London, 1892.

[xi] Levenspiel, O, and Chan, R.T. US-PS 4,408,656.

[xii] Feros Patenter Aktiebolaget FR-PS 2,507,290.

[xiii] Corman, J.C. and McLaughlin, M.H., Thermal Development of Heat Pipe Cooled I.C. Packages. ASME Paper 72-WA/HT-44, 1972.

[xiv] Grover, G.M. Evaporation-Condensation Heat Transfer Device. US Patent 3229759. Published 18 January, 1966.

[xv] Daverall, J.E., and Kemme, J.E. Satellite Heat Pipe. USAEC Report LA-3278, Contract W-7405-eng-36. Los Alamos Scientific Laboratory, University of California, Sept., 1970.

[xvi] Cheung, H. A Critical Review of Heat Pipe Theory and Applications. USAEC Report UCRL-50453. Lawrence Radiation Laboratory, University of California, 1968.

[xvii] Feldman, K.T., and Whiting, G.H. The Heat Pipe and its Application. Engrs. Dig., London, vol.28, No.3, pp 86-96, 1967.

[xviii] Eastman, G.Y. The Heat Pipe. Scientific American, vol. 218, No.5, pp 38-46, 1968.

[xix] Feldman, K.T., and Whiting, G.H. Application of the Heat Pipe. Mech. Engng., Nov., Vol.90, pp 48-53, 1963

[xx] Kay, J. and Mucciardi, F., "Software for the Modeling of Heat Pipe Injection Lances", Proc. of Sym. on Computer Software for Extractive Metallurgical Processes, CIM, pp. 215-225, 1993.

[xxi] Bullerschen, K.G. and H. Wilhelmi. Cooling of Arc Furnace Electrodes with Heat Pipes. Chem. Eng. Technol. 14 (1991) 45-53.

[xxii] Kirkpatrick, M.E., US-PS 3,667,329.

[xxiii] Choi, H., "Techniques for the Continuous Measurement of Melt Temperature", P. Eng. Thesis, McGill University, 1991.

[xxiv] Meratian, M., Mucciardi, F. and Gruzleski, J.E., "Novel Probe for the Thermal Analysis of Aluminum Alloys", Proc. Conf. International Symposium on Light Metals Processing and Applications, Quebec City, Canada, August 29 - September 1, 1993. pp. 315-324.

[xxv] Meratian, M., Mucciardi, F. and Gruzleski, J.E., "Thermal Analysis of Aluminum Casting Alloys with a Novel Heat Pipe Probe. Proceedings of the Light Metals Committee of the 123rd TMS Annual Meeting, San Francisco. Feb. 27 - March 3, 1994.

[xxvi] Gruzleski, J.E., and Closset, B.M., The Treatment of Liquid Al-Si Alloys, The American Foundrymen's Society, Inc., 1990, pp. 213-235.

[xxvii] Shibasaki, T., and Hayashi, H., Top-Blown Injection Smelting and Converting: The Mitsubishi Process. JOM, September, 1991, pp 20-26.

[xxviii] Moto Goto, The Mitsubishi Continuous Process: Operation and Design, Mitsubishi Metal Corp., Tokyo, Japan, February, 1988.

[xxix] Mast, E., Brown, M. and Mucciardi, F., Self-Cooled Heat Pipe Injection Lance, Canada and U.S. patents pending. U.S. Patent Application SN929748 filed in 1992 and granted in 1994.

[xxx] Mucciardi, F., Jin, N. and Kay, J., The Cooling of BOF Steelmaking Lances, 1994 Conference of the Iron and Steelmaking Society, Chicago, March 21-23, 1994.

[xxxi] Ohashi, Nobuo, "Modern Steelmaking", American Scientist, Volume 80, Nov.-Dec., 1992. pp. 540-555.

xxxii Mucciardi, F. Cooling in the Flat Rolling of Steel Products. Proc., 35th MWSP Conference, ISS-AIME, 1993.

xxxiii Ernst, D.M., and Eastman, G.Y., "High Temperature Heat Pipe Technology at Thermacore - An Overview," AIAA-85-0981. Presented at the AIAA 20th Thermophysics Conference, Williamsburg, Virginia, June 1985.

xxxiv Silverstein, C., Design and Technology of Heat Pipes for Cooling and Heat Exchange, Hemisphere Publishing Corp., Washington, 1992.

xxxv Kay, J., Eliminating Solid Phase Precipitation in High Temperature Thermosyphon Injection Lances Using a Na-K Liquid Solution, A F*A*C*T Project. Internal Report Prepared for Course MET 6209, Ecole Polytechnique, Dec., 1993

xxxvi Peterson, G.B., Bage, B.K., Entrainment Limitations in Thermosyphons and Heat Pipes, Journal of Energy resources Technology, Sept. 1991, Vol. 113, pp. 147-153.

xxxvii Farber, E.A., and E.L. Scorah, Heat Transfer to Water Boiling Under Pressure, Transactions of ASME, vol. 70, p.369, 1948.

xxxviii Baliga, R., Course notes for graduate level heat transfer course 305-650, McGill University, Montreal. February, 1992.

xxxix Zuber, N., "On the Stability of Boiling Heat Transfer", Trans ASME, vol. 80, p. 711, 1958.

xl Edwards, D.K. and B.D. Marcus, 1972, "Theory and design of Variable Conductance Heat Pipes: Steady State and Transient Performance," NASA CR-114530.

xli Strel'tsov, A.I. Theoretical and Experimental Investigation of Optimum Filling for Heat Pipes. Proc. 5th Int. Heat Transfer Conference, Japan; Vol. 5, Paper HE 2.3, 1974.

xlii Rohsenow, W.M., "Boiling", in Handbook of Heat Transfer (Eds., W.M. Rohsenow and J.P. Hartnett), Chap. 13, McGraw-Hill, N.Y., 1973.

xliii Holman, J.P. Heat Transfer (7th Edition). McGraw Hill, New York, 1990.

xliv Nusselt, W.: Die Oberflachenkondensation des Wasserdampfes, *VDI* Z., vol. 60, p. 541, 1916.

xlv Peterson, P.F. and C.L. Tien, 1990, "Mixed Double-Diffusive Convection in Gas-Loaded Heat Pipes," ASME Journal of Heat Transfer, Vol. 112, Feb., 1990, pp. 78-83.

xlvi Hijikata, K., S.J. Chen and C.L. Tien, 1984, "Non-Condensable Gas Effect on Condensation in a Two-Phase Closed Thermosyphon," International Journal of Heat and Mass Transfer, Vol. 27, pp. 1319-1325.

xlvii Peterson, P.F. and C.L. Tien, 1989, "Numerical and Analytical Solutions for Two-Dimensional Gas Distribution in Gas-Loaded Heat Pipes," ASME Journal of Heat Transfer Vol. 111, pp.598-604.

[xlviii] Van der Vooren, J., A.A.M. Delil and A. Sanderse, June, 1980, "Uniaxial model for a Gas-Loaded Variable Conductance Heat Pipe," National Aerospace Laboratory Report NLR TR 80048U, Amsterdam.

[xlix] Bobco, R.P., 1987, "Variable Conductance Heat Pipes: A First Order Model," Journal of Thermophysics and Heat Transfer, Vol. 1, pp.35-42.

[l] Edwards, D.K. and B.D. Marcus, 1972 "Heat and Mass Transfer in the Vicinity of the Vapor-Gas Front in a Gas-Loaded Heat Pipe," ASME Journal of Heat Transfer, vol. 94, pp. 155-162.

[li] Coscia, Carlo, "Mathematical Modeling of an Annular Heat Pipe," Undergraduate Thesis for course 306-497B, 1992, Department of Metallurgical Engineering, McGill University, Canada.

[lii] Bobco, R.P., 1989, "Performance Prediction: Comparison of First-Order and Flat-Front Models," Journal of Thermophysics and Heat Transfer v3 n4 Oct 1989 pp 401-405

[liii] Peterson, Fredrick, "Diffusion and Convection of Noncondensables in Heat Pipe Condensation," Ph.D thesis, Mech. Eng., 1988, University of California, Berkeley.

[liv] Gross, U., Reflux condensation heat transfer inside a closed thermosyphon, International Journal of Heat and Mass Transfer v 35, n 2, Feb. 1992, pp. 279-294

[lv] Kobayashi, Y. and A. Okumura, Effect of gravity and noncondensable gas levels on condensation in variable conductance heat pipes, Journal of Thermophysics and Heat Transfer, V.5, N.1, Jan 1991, pp. 61-68.

[lvi] Press, W. H., 1992, *Numerical Recipes in FORTRAN*, 2nd Ed, Cambridge University Press, p. 372.

[lvii] Macabuag, Y., 1994, *Application of an Annular Thermosyphon as a Self-Cooling Injection Lance: Effects of Inert Gas Loading*, Undergraduate Research Report, Department of Mechanical Engineering, McGill University, Canada.

[lviii] Yip, Chisan, 1993, *Application of a Heat Pipe as a Depth Gauge*, Undergraduate Research Report, Department of Mechanical Engineering, McGill University, Canada.